United States Department of Commerce
Technology Administration
National Institute of Standards and Technology

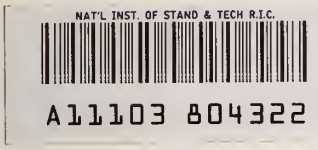

NIST Technical Note 1293

A Mathematical Model of Cathodic Delamination and Blistering Processes in Paint Films on Steel

James Pommersheim, Tinh Nguyen, Zhuohong Zhang, Changjian Lin, Joe Hubbard

The National Institute of Standards and Technology was established in 1988 by Congress to "assist industry in the development of technology . . . needed to improve product quality, to modernize manufacturing processes, to ensure product reliability . . . and to facilitate rapid commercialization . . . of products based on new scientific discoveries."

NIST, originally founded as the National Bureau of Standards in 1901, works to strengthen U.S. industry's competitiveness; advance science and engineering; and improve public health, safety, and the environment. One of the agency's basic functions is to develop, maintain, and retain custody of the national standards of measurement, and provide the means and methods for comparing standards used in science, engineering, manufacturing, commerce, industry, and education with the standards adopted or recognized by the Federal Government.

As an agency of the U.S. Commerce Department's Technology Administration, NIST conducts basic and applied research in the physical sciences and engineering and performs related services. The Institute does generic and precompetitive work on new and advanced technologies. NIST's research facilities are located at Gaithersburg, MD 20899, and at Boulder, CO 80303. Major technical operating units and their principal activities are listed below. For more information contact the Public Inquiries Desk, 301-975-3058.

Technology Services
- Manufacturing Technology Centers Program
- Standards Services
- Technology Commercialization
- Measurement Services
- Technology Evaluation and Assessment
- Information Services

Electronics and Electrical Engineering Laboratory
- Microelectronics
- Law Enforcement Standards
- Electricity
- Semiconductor Electronics
- Electromagnetic Fields[1]
- Electromagnetic Technology[1]

Chemical Science and Technology Laboratory
- Biotechnology
- Chemical Engineering[1]
- Chemical Kinetics and Thermodynamics
- Inorganic Analytical Research
- Organic Analytical Research
- Process Measurements
- Surface and Microanalysis Science
- Thermophysics[2]

Physics Laboratory
- Electron and Optical Physics
- Atomic Physics
- Molecular Physics
- Radiometric Physics
- Quantum Metrology
- Ionizing Radiation
- Time and Frequency[1]
- Quantum Physics[1]

Manufacturing Engineering Laboratory
- Precision Engineering
- Automated Production Technology
- Robot Systems
- Factory Automation
- Fabrication Technology

Materials Science and Engineering Laboratory
- Intelligent Processing of Materials
- Ceramics
- Materials Reliability[1]
- Polymers
- Metallurgy
- Reactor Radiation

Building and Fire Research Laboratory
- Structures
- Building Materials
- Building Environment
- Fire Science and Engineering
- Fire Measurement and Research

Computer Systems Laboratory
- Information Systems Engineering
- Systems and Software Technology
- Computer Security
- Systems and Network Architecture
- Advanced Systems

Computing and Applied Mathematics Laboratory
- Applied and Computational Mathematics[2]
- Statistical Engineering[2]
- Scientific Computing Environments[2]
- Computer Services[2]
- Computer Systems and Communications[2]
- Information Systems

[1] At Boulder, CO 80303.
[2] Some elements at Boulder, CO 80303.

NIST Technical Note 1293

A Mathematical Model of Cathodic Delamination and Blistering Processes in Paint Films on Steel

James Pommersheim *
Tinh Nguyen
Zhuohong Zhang *
Changjian Lin **
Joe Hubbard

* Chemical Engineering Department, Bucknell University, Lewisburg, PA

** Present Address:
Chemistry Department
Xiamen University, Fujian,
People's Republic of China

Building and Fire Research Laboratory
National Institute of Standards and Technology
Gaithersburg, MD 20899

May 1992

U.S. Department of Commerce
Barbara Hackman Franklin, Secretary

Technology Administration
Robert M. White, Under Secretary for Technology

National Institute of Standards and Technology
John W. Lyons, Director

National Institute of Standards
and Technology
Technical Note 1293
Natl. Inst. Stand. Technol.
Tech. Note 1293
72 pages (May 1992)
CODEN: NTNOEF

U.S. Government Printing Office
Washington: 1992

For sale by the Superintendent
of Documents
U.S. Government Printing Office
Washington, DC 20402

Abstract

Conceptual and mathematical models are developed for processes which describe blistering of defect–containing coating on coated steel containing defects exposed to electrolytic solutions. The assumption is made that cations migrating along the coating/metal interface from an anode at the defect to cathodic sites are responsible for blistering. The cations are driven by both concentration and electrical potential gradients. The mathematical models are solved to predict ion fluxes and concentrations along the interface and within the blister. Solutions of the models are expressed in terms of dimensionless parameters. Model variables include blister size, distance between the blister and defect, ion diffusivity and potential gradients. To substantiate the models, an experiment was designed and conducted to measure the transport of cations along the coating/metal interface from the defect to the blister. Sodium ion concentration–time data within a blister were analyzed to determine model parameters. Under the experimental conditions employed, it was found that the transport of sodium ions is controlled by potential gradients rather than concentration gradients. Model results indicate that large blisters subject to a potential gradient are more likely to grow than small ones because higher concentrations can build up within them. Implications of this conclusion for maintaining the integrity of organic coatings are discussed.

keywords: anode, blistering, cathode, cathodic delamination, conceptual model, corrosion, defect, diffusion, mathematical model, organic coatings, paint films, potential gradients, scribe

Table of Contents

Table of Figures

1. Introduction

Corrosion of metals costs the United States about 4.2% of the gross national product yearly [1]. The use of organic coatings is an effective, economical, and widely used method to prolong the service life of metals. The coatings are barriers which help prevent metals from corroding, and protect the substrate from both chemical and physical attack. Despite recent improvements in coating technologies, problems continue to exist in providing protection for metals from exposure to potentially corrosive environments.

One of the major problems of coating technology is osmotic blistering. When foreign ions are present on the surface or leachable ions are present in the coating, the substrate will not be clean. In the presence of microscopic amounts of water, local osmotic cells or blisters can be established on unclean substrates [2]. Blistering is considered to initiate at the metal–substrate interface at weak spots randomly distributed over the substrate surface. Blister growth occurs when there is sufficient water present in the vicinity of the metal substrate. Osmotically driven diffusion of water through the coating controls the rate of growth. One of the most severe forms of blistering is cathodic blistering which can occur when a coated metal with defects in the coating is exposed to a deleterious environment, for example, when the coating is exposed to salt spray or is immersed in a salt solution. The high pH within cathodic blisters has been postulated to cause the delamination of the coating from the metal at the blister periphery [3–5]. After sufficient time, the blisters may enlarge to a point where adjacent blisters coalesce. This can lead to complete detachment of the coating from the substrate causing premature failure of the organic coating system by delamination.

Although considerable research on the degradation and adhesion failure of coatings has been done in the past decade [6,7], little work has been done to quantify the cathodic delamination and blistering processes. Quantitative study is necessary to predict the performance of a given coating system in order to obtain estimates of service life. One reason for the difficulty in quantifying the delamination and blistering processes is the complexity of the metal/coating system. Many variables affect the performance and service life of coating systems. In addition to the physical and chemical properties of the coating and the substrate surface, a coating system may contain inhomogeneities such as air bubbles, microvoids and trapped solvent. Also the coating may be applied to previously poorly bonded or nonbonded areas. These factors influence the transport of deleterious species through the coating and along the metal/coating interface and can promote degradation at the interface. Another reason for the lack of a comprehensive theory for understanding and predicting corrosion protection by a coating is that many different coating formulations are currently employed.

If the effectiveness of coatings is to be increased through development of improved selection and evaluation criteria, it is essential to develop improved methods for predicting the service life of a coated metal.

In this paper, conceptual and mathematical models are developed for the rate at which sodium ions are transported from the environment to cathodic blisters in a coating/metal system. Transport occurs due to the combined effect of diffusion and an electrical field created by an applied potential gradient. Expressions are obtained for the sodium ion flux into a blister and the concentration profile between a blister and its environment. By comparing model predictions with experimental data of sodium ion concentration versus time, the controlling mechanism for ion transport is determined.

2. Conceptual Model: Description of the Blistering Process

The degradation of an "intact" coating on steel immersed in electrolytes can proceed by the following steps:

1. Coating swelling, polymer conformation change, or pigment percolation (clustering) result in enlargement or formation of pathways for electrolyte migration to the metal surface. This can be seen by electrochemical and spectroscopic measurements [8,9].
2. Corrosion occurs at the base of the pathway which acts as an anode. This oxidation reaction supplies electrons for the cathodic reactions, which occur away from the anode and underneath the coating.
3. Cations migrate to the cathodic sites to neutralize the hydroxide ion, forming highly alkaline and hygroscopic materials. The migration of cations also induces an electro–osmotic flow of water to the cathodic sites.
4. Alkaline solution causes coating/metal interfacial delamination around the initial blister, which is cathodic.
5. Hygroscopic materials result in a thermodynamic water activity difference between the inside and outside of the blister.
6. Osmotic and electro–osmotic pressure differences control the growth rate of blisters.
7. Alkalinity of blister solution and mechanical stress facilitate can add to the enlargement process.

Cathodic blistering occurs in the neighborhood of coating defects. Continued exposure to salt spray, constant immersion, or cyclic wet–dry immersion in electrolytes will lead to enlargement, or a coalescence of the blisters, and eventual total delamina-

tion of coatings. The growing anodic character at the defect area stimulates the cathodic reactions adjacent to it. Cathodic blistering also occurs when an electric potential is applied across the coated panels. Many coated metals are intentionally or unintentionally subjected to an electrical potential.

The defect serves as the anode where the iron is oxidized by the half–cell reaction:

$$Fe \text{ ----> } Fe^{2+} + 2e^{-} \ .$$

The other half cell corrosion reaction, where the oxygen is reduced (the cathodic reaction), occurs under the coating a short distance away from the defect [3]:

$$H_2O + 1/2O_2 + 2e^{-} \text{ ----> } 2OH^{-} \ .$$

The cathodic and anodic sites are connected by an electrolyte layer. Initially the cathodic and anodic reaction can start at adjacent atomic sites. However, as corrosion products form and concentration gradients of corrosive species are established, the reaction sites separate and localize. An increase of this separation can lead to delamination failure. The liquid in cathodic blisters exposed to dilute salt solution is highly alkaline, while the liquid in neutral blisters under defect–free organic coatings is weakly acidic to neutral [10].

Although there are many factors that affect the concentration of the solution in the blister and the rate of the cathodic reaction, two main factors are considered paramount. One is the applied potential and the other is diffusion. Both act to transport ions in the electrolytic solution from the anode and to the cathode. Mathematical models are developed here to describe these phenomena and their interaction.

Figure 1 presents a schematic of the model system for cathodic blistering. The figure shows a physical model of a coating/metal system exposed to a NaCl solution

and gives the route taken by the sodium ions. There is a central blister in the coating of radius "a", and a defect (scribe) located at a distance R from the blister. A path is provided between the blister and scribe beneath the coating film by a channel whose effective width is δ. As depicted, the sodium ions will enter the channel through the scribe to reach the blister. The mechanism for ion transport is diffusion in the presence of an imposed electrical field. The movement of sodium ions from the scribe to the blister can be divided into two sequential stages: an initial period and a propagation period.

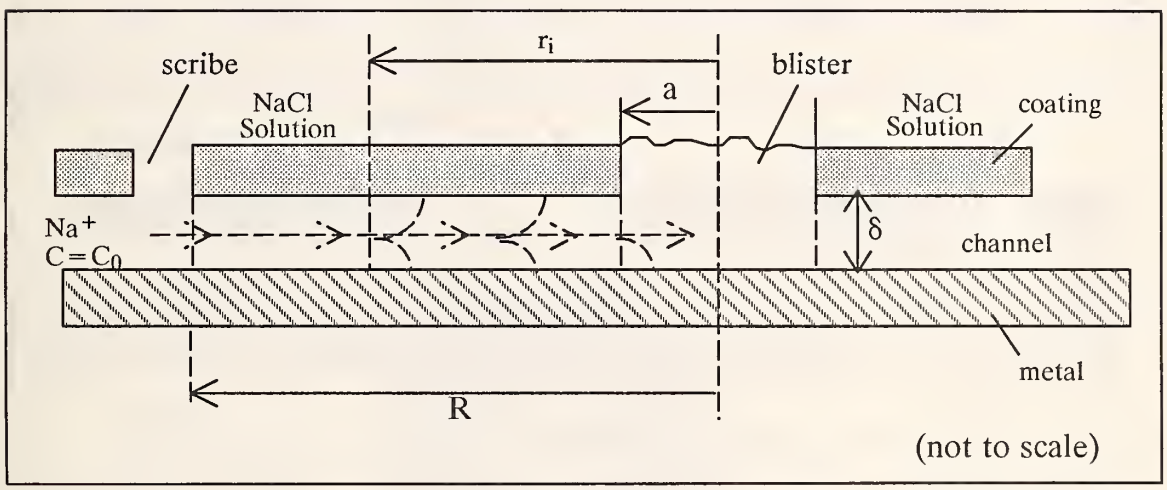

Figure 1. Conceptual Model for Initial Period .

Figure 1 presents a profile of the model system during the initial period. In the conceptual model adsorption on the wall of the channel is assumed to be instantaneous compared to diffusion and charge transfer. It is assumed that the metal surface within the channel is in the cathodic state and that the electrolyte layer in the channel is alkaline. These assumptions are consistent with Step 2 of the conceptual model. Under these conditions, the fixed charges on the metal and the coating surface within the channel are negative [11]. Consequently, cations are adsorbed on these sites. If

the adsorption is rapid, the concentration of sodium ions will drop to near zero at the advancing interface (located at a distance r_i from the center of the blister solution). The concentration of sodium ions within the blister will remain near background levels during the initial stage as a moving interface travels in the channel between the scribe and blister. The time taken for the interface to reach the blister periphery ($r_i = a$) is the initiation or break through time, Θ_i. This is the time it takes sodium ions to first reach the blister site. The quasi-steady state assumption maintains that there is no additional depletion of sodium ions within the channel as the interface advances to reach the blister. This is a reasonable assumption considering the large reservoir of sodium ions in the external solution that are available for transport.

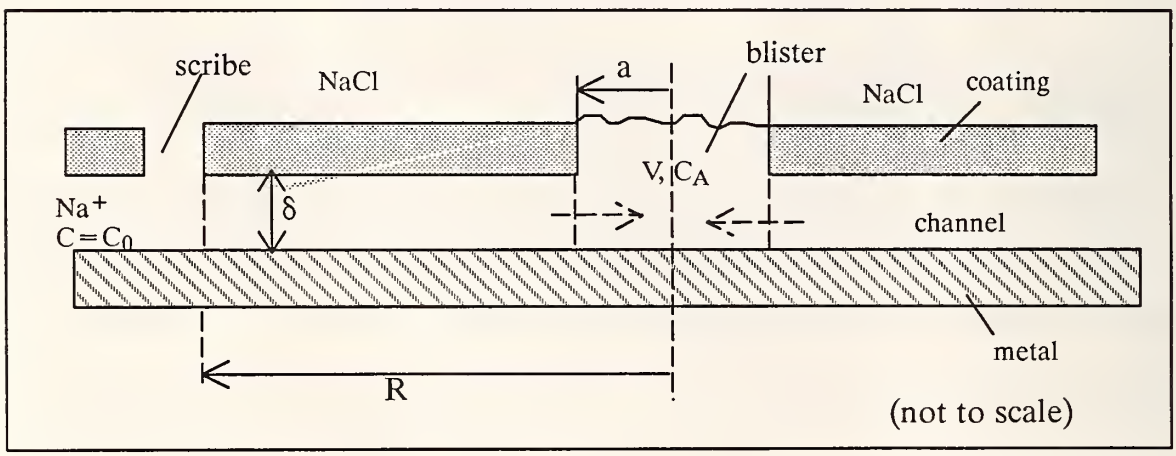

Figure 2. Conceptual Model for Propagation Period .

Figure 2 presents a profile of the model system during the propagation period. The propagation period occurs at longer times ($t > \Theta_i$), after the sodium ions have broken through into the blister. Sodium ions are no longer removed in the channel but can now pass freely into the blister. In this stage, ions enter the blister as a result of both diffusion and transport caused by the applied electric field. Ions accumulate within the blister but no longer within the channel. Their concentration C_A will rise within the blister during this period.

3. Mathematical Model Development

3.1 Review of Related work

Nguyen *et al* [12] developed a mathematical model for the cathodic blistering of protective coatings containing detects on steel immersed in electrolytes. Their model was based on two basic assumptions: 1) metal cation presence at the cathodic sites is the main factor controlling the thermodynamic activity of water across the coating, and 2) lateral diffusion along the coating/metal interface from the defects to the blisters is the main route of cation transport. The model predicts the concentration profiles and cation flux flowing into a blister as a function of time, blister size, distance between the blister and defect, ion diffusivity and potential gradient.

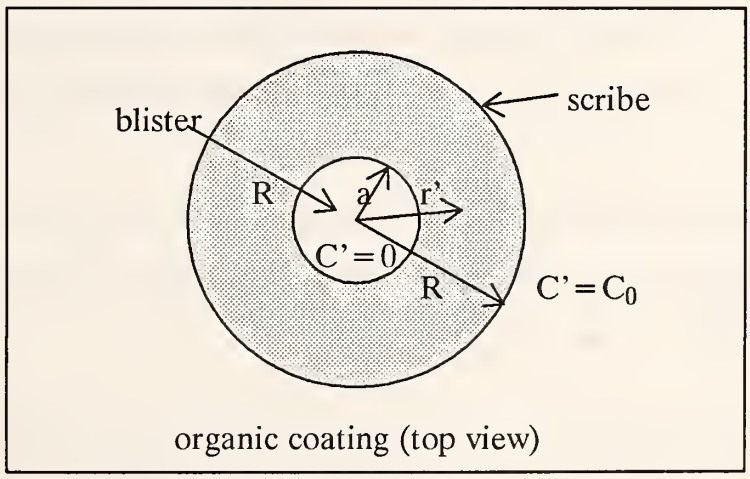

Figure 3. Model System for Cathodic Blistering [12] .

The model is based on two-dimensional, radially symmetric diffusion in an annular domain, $a < r' < R$. Figure 3 presents a top view of the model system. a is the radius of the blister, R is the distance between the center of the blister and the

scribe (defect), and r' is the distance between the center of the blister and any site on the coated panel between the blister and the scribe. C' is the sodium ion concentration at any site on the coated panel between the blister and the scribe, and C_0 is the sodium ion concentration in the environment.

The cation is assumed to diffuse from the scribe to the blister along the coating/metal interface. The model developed by Nguyen *et al* [12] is given by:

$$\frac{\partial C'}{\partial t'} = D \frac{1}{r'} \frac{\partial}{\partial r'} \left(r' \frac{\partial C'}{\partial r'} \right) + \mu E \frac{\partial C'}{\partial r'} \qquad (1)$$

where t' is the exposure time, D is the effective sodium ion diffusion coefficient under the coating, μ is the average mobility of sodium ions and E is the strength of the imposed unscreened electrical field.

Equation (1) was rewritten in dimensionless units, in terms of a distance scale r, a time scale t and a concentration scale C [12]. The resulting dimensionless equation has the form:

$$\frac{\partial C}{\partial t} = \frac{\partial^2 C}{\partial^2 r} + \frac{1}{r} \frac{\partial C}{\partial r} + \frac{p}{r} \frac{\partial C}{\partial r} \qquad (2)$$

with

$$C = \frac{C'}{C_0}, \quad t = \frac{Dt'}{L^2}, \quad r = \frac{r'}{R-a}, \quad p = \frac{-\mu\,(\Delta\Phi)}{D \log\left(\frac{1}{k}\right)} \quad \text{and} \quad k = \frac{a}{R}$$

$\Delta\Phi$ is the potential difference between a and R, and L is the length scale (L=R–a).

The dimensionless boundary conditions are given by:

$$C\left(\frac{k}{1-k},\ t\right) = 0 \tag{3}$$

$$C\left(\frac{1}{1-k},\ t\right) = 1 \tag{4}$$

$$C(r,\ 0) = 0\,. \tag{5}$$

Condition (3) corresponds to the fact that the sodium ion concentration at the blister periphery is zero at any time. This condition is more likely to obtain for larger blisters or at shorter times where the sodium ion concentration remains low. At the scribe, condition (4) shows that the concentration is constant at C_0. Condition (5) corresponds to the fact that initially there are no sodium ions beneath the coating.

The dimensionless cation flux F flowing into the blister is given by:

$$F = -\frac{2\pi k}{1-k}\left(\frac{\partial C}{\partial r}\right)_{r\,=\,k/(1-k)}\,. \tag{6}$$

Nguyen *et al* [12] solved the above set of equations numerically. They presented graphical results of the dimensionless concentration and flux as functions of system parameters.

There are two dimensionless parameters in this problem: the geometric aspect ratio k and the dimensionless potential gradient p. High p means the applied electric field in the region between the blister and scribe is large, while low p means the electric field is small.

It is noted here that since the transfer of sodium ions is caused by both an electric field and diffusion, the time scale is not determined solely by the dimensionless diffu-

sion time $t' = tD/(R-a)^2$ since the time scale associated with the electric field must also be considered.

3.2 Steady State Ion Concentration Profile and Flux

In this section the steady state ion concentrations and fluxes are derived for the model of Nguyen *et al* [12].

The dimensionless concentration profile for the diffusing cation are governed by eq (2). At steady state this equation becomes:

$$\frac{d^2C}{dr^2} + \frac{1}{r}\frac{dC}{dr} + \frac{p}{r}\frac{dC}{dr} = 0 . \qquad (7)$$

The boundary conditions are still given by eqs (3) and (4). Application of these conditions to eq (7) results in the following analytical solutions in the absence ($p = 0$) and presence ($p \neq 0$) of an applied electric field:

$$C(r) = \frac{1}{\ln k} \ln\left[\frac{\left(\frac{k}{1-k}\right)}{r}\right] \qquad (for\ p = 0) \qquad (8)$$

$$C(r) = \frac{1}{1-k^p}\left[1 - \left(\frac{\frac{k}{1-k}}{r}\right)^p\right] \qquad (for\ p \neq 0) . \qquad (9)$$

When $p = 0$, there is no applied potential and diffusion is the sole mechanism for ion transport. Equation (9) can be shown to reduce to eq (8) in the limit as $p \rightarrow 0$.

Application of eq (6) to eqs (8) and (9) results in the following equations for the dimensionless sodium ion flux when $p = 0$ and $p \neq 0$:

$$F = \frac{2\pi}{\ln k} \qquad (for\ p = 0) \tag{10}$$

$$F = \frac{2\pi p}{k^p - 1} \qquad (for\ p \neq 0)\ . \tag{11}$$

The fluxes are negative ($k < 1$) because ions are diffusing inward in the direction of decreasing radius. Equation (11) reduces to eq (10) in the limit as $p \rightarrow 0$.

3.3 Mathematical Models for the Initial and Propagation Period

In this section mathematical models are developed and solved for the initial and propagation periods of the conceptual model presented in section 2.

3.3.1. Model for the Initial Period ($t < \Theta_i$)

In this period, as previously described, the model presumes that a moving interface travels in the channel between the scribe and the blister. The time taken for the interface to reach the blister periphery is the initiation or break through time Θ_i. During this period eq (7) describes the facilitated transport of sodium ions. The boundary conditions are $C' = 0$ at $r = r_i$ and $C' = C_o$ at $r = R$. C_o, the concentration of sodium ion in the external solution, is presumed constant in the present formulation. The solutions for the quasi–steady state concentration profile and flux are similar to those obtained previously at steady state. If a is replaced by r_i, with k_i defined as r_i/R, then the mathematics can be transposed directly. Thus, the dimensionless concentration profile and flux in the absence of an electric field ($p = 0$) are given by eqs (12) and (13), respectively:

$$C = \frac{C'}{C_0} = \frac{\ln\left(\frac{r_i}{r'}\right)}{\ln k_i} \qquad (for\ p = 0) \qquad (12)$$

$$F = \frac{2\pi}{\ln k_i} \qquad (for\ p = 0) \qquad (13)$$

The dimensionless concentration profile and flux in the presence of an electric field ($p \neq 0$) are given by eqs (14) and (15), respectively :

$$C = \frac{C'}{C_0} = \frac{1 - \left(\frac{r'}{r_i}\right)^p}{1 - k_i^p} \qquad (for\ p \neq 0) \qquad (14)$$

$$F = \frac{2\pi p}{k_i^p - 1} \qquad (for\ p \neq 0)\ . \qquad (15)$$

As described in the conceptual model, at $r = r_i$ an instantaneous adsorption or reaction process is assumed to immobilize the sodium ion. Because this process is rapid the local concentration of sodium ions will be low. In this case the ion transport due to the applied electric field will also be low and the total moles flow at $r = r_i$ will approximate the diffusive molar flow. The diffusive molar flow w_d (mol/s) of sodium ion is given by:

$$w_d = -\bar{\varrho}_s \frac{dr_i}{dt}\, 2\pi r_i \qquad (16)$$

where $\bar{\varrho}_s$ is the amount of adsorbed sodium per unit of interfacial area (mol/m^2).

it will be a constant which only depends on temperature and the nature of the adsorbate–adsorbent system. Another expression for w_d is given by the product of the flux and the transport area:

$$w_d = - D \left(\frac{\partial C'}{\partial r'} \right)_{r'=r_i} 2\pi r_i \, \delta \, . \tag{17}$$

Equating eqs (16) and (17):

$$- \frac{dr_i}{dt} = \frac{D \, \delta}{\tilde{\varrho}_s} \left(\frac{\partial C'}{\partial r'} \right)_{r'=r_i} . \tag{18}$$

In the presence of an electric field ($p \neq 0$) the concentration derivative can be found from eq (14), when:

$$\frac{dr_i}{dt} = \frac{D \, \delta}{\tilde{\varrho}_s} \frac{C_0 \, p}{r_i} \frac{1}{\left(\frac{r_i}{R}\right)^p - 1} \tag{19}$$

eq (19) predicts the rate at which the interface moves in from the scribe to the blister.

Separating variables and integrating eq (19) from $r = R$ to $r = r_i$, it follows that:

$$\frac{1}{p+2} \left(\frac{r_i}{R} \right)^{p+2} - \frac{1}{2} \left(\frac{r_i}{R} \right)^2 - \frac{1}{p+2} + \frac{1}{2} = \alpha' p t \quad (\textit{for } p \neq 0) \tag{20}$$

where

$$\alpha' = \frac{D \, \delta}{\tilde{\varrho}_s} \frac{C_0}{R^2} \, . \tag{21}$$

The initiation or break through time Θ_i occurs when $r_i = a$, so that:

$$\Theta_i = \frac{1}{\alpha' \, p} \left[\frac{1}{p+2} \, k^{p+2} - \frac{1}{2} \, k^2 - \frac{1}{p+2} + \frac{1}{2} \right] \quad (\textit{for } p \neq 0) \, . \tag{22}$$

In the absence of an electric field, p = 0, we obtain by a similar procedure:

$$\frac{dr_i}{dt} = \frac{D\,\delta}{\tilde{\varrho}_s}\,\frac{C_0}{r_i}\,\frac{1}{\ln\frac{r_i}{R}}\,. \tag{23}$$

Integrating similarly, it follows that:

$$\left(\frac{r_i}{R}\right)^2 \ln\left(\frac{r_i}{R}\right) - \frac{1}{2}\left(\frac{r_i}{R}\right)^2 + \frac{1}{2} = 2\,\alpha'\,t\,, \qquad (for\ p = 0)\,. \tag{24}$$

The break through time when p = 0 is given by:

$$\Theta_i = \frac{1}{2\,\alpha'}\left[k^2\left(\ln k - \frac{1}{2}\right) + \frac{1}{2}\right], \qquad (for\ p = 0)\,. \tag{25}$$

Using eqs (22) and (25), respectively, the break through time Θ_i taken for cations to first reach the blister periphery can be calculated with ($p \neq 0$) and without ($p = 0$) an applied potential gradient.

3.3.2. Model for the Propagation Period ($t > \Theta_i$)

As shown in figure 2, once the moving interface has reached the periphery of the blister ($r_i = a$), additional sodium ion will enter due to a combination of diffusion and transport caused by the electric field. The propagation period begins when the initial period ends (at $t = \Theta_i$).

A sodium balance made on the blister in this stage takes the form:

$$\frac{d}{dt}(VC_A) = w_d\big|_{r'=a} + w_e\big|_{r'=a} \tag{26}$$

where w_e is the molar flow caused by the electric field, V is the volume of solution in the blister and C_A is its concentration.

Equation (17) provides an expression for the diffusion flow, while the electric field flow is given by:

$$w_e = 2\pi \mu \Delta\Phi \delta \frac{k/(1-k)}{\ln(1/k)} C' . \quad (27)$$

The flux, F_e, caused by the electric field is obtained by dividing by the transport area of the blister periphery, i.e., $2\pi a\delta$:

$$F_e = \frac{\mu \Delta\Phi}{(R-a) \ln k} C' . \quad (28)$$

These results show that the electrical flow and flux are both proportional to the concentration C′.

Combining the diffusion flow (eq (17)) and the ion flow induced by the electric field (eq (27)):

$$\frac{d}{dt}(VC_A) = V\frac{dC_A}{dt} = -D\left(\frac{\partial C'}{\partial r'}\right)_{r'=a} 2\pi a \delta + 2\pi \mu \Delta\Phi \delta \frac{k/(1-k)}{\ln(1/k)} C' . \quad (29)$$

This formulation presumes that the volume of solution V in the blister remains constant (fig. 3). Since $\Delta\Phi$ is negative (potential gradient is inward), p will be positive when the blister is cathodic.

At quasi-steady state, there is no additional depletion of sodium ions under the coating ($\partial C'/\partial t = 0$), and all of the ions which pass under the film arrive in the blister. The quasi-steady state assumption is reasonable considering the generally small volume of solution under the film relative to the volume of solution in the blister. Also during the initial period the coating has ample time to adsorb sodium ions. In this

case the total molar flow of sodium ions, as expressed by the right hand side of eq (26), will be constant. Evaluating this constant at $r' = a$, and using eq (29), it follows that:

$$\frac{dC_A}{dt} = \frac{2\pi\ \delta\ D}{V \ln(1/k)} \left[C_0 - C_A \left(1 - \frac{k\ (\ln 1/k)}{1-k}\ p \right) \right] . \tag{30}$$

Integrating again provides an expression for the concentration of sodium ions within the blister as a function of time during the propagation period:

$$\frac{C_A}{C_0} = \frac{1}{\alpha} \left[1 - e^{-\alpha \beta (t-\Theta_i)} \right] \tag{31}$$

where

$$\alpha = 1 - \frac{k \ln(1/k)}{1-k}\ p = 1 - \left(\frac{p}{p^*} \right) \tag{32}$$

and

$$\beta = \frac{2\pi\ \delta\ D}{V \ln(1/k)} \tag{33}$$

with

$$p^* = \frac{1-k}{k \ln(1/k)} \tag{34}$$

p^* is defined as the critical value of the dimensionless electric field. Note that when $p = p^*$, $\alpha = 0$. p^* is solely a function of the aspect ratio k. Therefore, it depends on the relative size of the blister and the separation of the anodic and cathodic regions.

The model predicts that what occurs within the blister will depend on the relative values of p and p^*. There are three possible cases: $p < p^*$, $p > p^*$ and $p = p^*$. The

three types of concentration–time profiles which can result for these cases are depicted in figure 4.

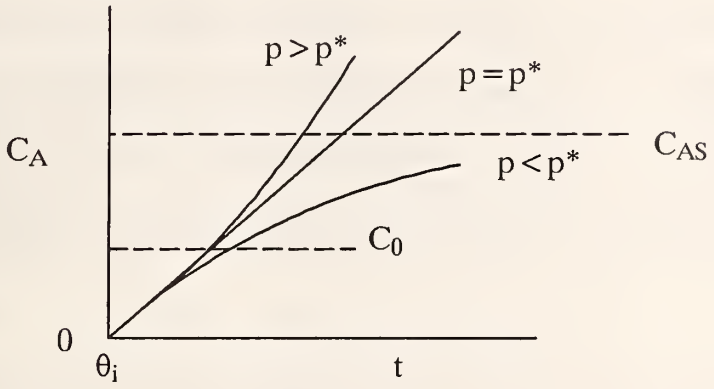

Figure 4. The Three Types of Predicted Cation Concentration–Time Profiles in a Blister .

If $p < p^*$, α is positive, and a steady state concentration C_{AS} within the blister is reached, C_{AS} is given by:

$$\frac{C_{AS}}{C_0} = \frac{1}{1 - \frac{k \ln(1/k)}{1-k} p} \cdot \tag{35}$$

C_{AS} is predicted to be higher than C_o so long as the blister remains cathodic with respect to the scribe, that is, $p > 0$. The lower curve in figure 4 depicts this behavior. In the absence of an electric field ($p = 0$), the steady state value will reach the concentration of sodium ions in the external solution.

If $p > p^*$, α is negative, and the concentration is predicted to increase without limit. In this case eq (31) can be written:

$$\frac{C_A}{C_0} = \frac{e^{|\alpha\beta|\,(t-\Theta_i)} - 1}{|\alpha|} \quad . \tag{36}$$

Here, a steady state concentration of sodium ions within the blister is not reached. The concentration is predicted to increase indefinitely so long as sodium ions are available for transport, so that concentrations within the blister can be many times the external solution concentration. This behavior is illustrated by the upper curve in figure 4.

For the special case when $p = p^*$, $\alpha = 0$, and the concentration within the blister is predicted to increase linearly with time according to:

$$C_A = \beta\, C_0\, (t - \Theta_i) \quad . \tag{37}$$

This is shown by the inclined straight line in figure 4.

The parameters α and β can be evaluated by fitting experimental data to one of eqs (35), (36), and (37). Further, the parameter p can be calculated from the best value of α using eq (32).

The approach to steady state depends on the system time constant $\tau = 1/\alpha\beta$ given by:

$$\tau = \frac{V \ln(1/k)}{2\pi\, \delta\, D} \frac{1}{1 - p/p^*} = \frac{V \ln(1/k)}{2\pi\, \delta\, D} \frac{C_{AS}}{C_0} \quad . \tag{38}$$

Equation (38) presents the system time constant τ as a function of the steady state concentration. It shows that the time constant at each p is directly proportional to (C_{AS}/C_0). Positive values of τ only occur when $p < p^*$. A large diffusion coefficient

D gives a low time constant τ so that diffusion is more likely to control ion flow (p low). With a low diffusion coefficient, a high time constant will result and electric field control of flow (p high) is more likely. However, if p equals or exceeds p*, there is no time constant and the system never reaches a steady state. Since eq (30) is a first order linear differential equation, the time constant τ is equal to the time taken for the concentration to go 63.2% of the way from its initial to its final value C_o. The shortest time constant occurs when p is negative. This occurs when ions flow outward from the blister solution (counter–current flow). In this case the model solution predicts that the electric field opposes the diffusion process so that a low steady state concentration can be reached rather quickly. However such a situation is unlikely in practice because the blister would go from a cathodic to an anodic state, so that the corrosion reactions which sustain ion transport would occur elsewhere.

4. Experimental

To verify the models an experiment was designed and conducted to measure the diffusion of cations along the coating/metal interface from the defect to the blister. Experimental details are provided in this section.

4.1 Specimen Preparation

The specimen configuration for metal cation diffusion along the interface is schematically shown in figure 5. An SAE 1010 cold rolled steel panel (Q Panel•) with

---

•Certain commercial equipment is identified in this paper in order to specify adequately the experimental procedure. In no case does such identification imply recommendation or endorsement by the National Institute of Standards and Technology, nor does it imply that it is necessarily the best available for the purpose.

a dimension of 150 x 100 x 0.8 mm was used as the substrate. The specimen was prepared by making a 5 mm diameter perforation in the middle of an as-received, uncoated steel panel. The perforated panel was then glued to a 3.0 mm thick poly (methyl methacrylate) (PMMA) sheet using a room-temperature-cured epoxy adhesive. A hole of 2 mm diameter was drilled through the PMMA sheet near the center of the perforation. A 4 mm diameter disk of the same steel with a copper wire soldered to it was placed flat on the PMMA sheet at the center of the perforated space. The wire was then put through the PMMA sheet. Care was taken so that the surfaces of the disk and of the panel were approximately at the same level. The space between the 5 mm disk and the 4 mm perforation was filled with a room-temperature-cured epoxy. This epoxy insert served as an electrical insulator between the steel disk at the center and the rest of the steel panel.

The steel surface of the panel was sanded (sand paper grit no. 320) to produce a clean and flat surface. Prior to applying the organic coating, the sanded panel was repeatedly cleaned with methanol then dried with dry air. (A drop of distilled water spread spontaneously on the panel surface after cleaning, indicating that the surface was free of organic contaminants.) A commercial, high-build, room-temperature-cured epoxy coating was applied on the panel using the draw-down technique. The thickness of the dry coating was approximately 450 μm as measured by an eddy current gage. After curing for 1 week, a 5 mm diameter disk, of the coating from the same location where the perforation in the steel was made, was bored to the steel substrate and removed from the coated panel. A glass tube having an outside diameter of 4.5 mm and a height of 50 mm was placed where the coating disk had been removed. Epoxy adhesive was used to seal the space between the glass tube and coating. To ensure that the epoxy adhesive did not touch the steel surface and block the lateral diffu-

sion route, a hollow disk of tetrafluorethylene polymer having an outside diameter of 5 mm and inside diameter of 3 mm was situated at the bottom of the glass tube (refer to fig. 5). The glass tube assumes the function of a constant volume cathodic blister.

A circular scribe through the coating to the steel substrate was made around and away from the glass tube. The radius between the scribe and the center of the glass tube was 22.5 mm. The width of the scribe was 2 mm. The scribe provided a defect through which the cations could enter the system. An open-ended PMMA cylinder having a height of 50 mm and an inside diameter of 50 mm was placed symmetrically around the glass tube. For this configuration, the experimental value of the parameter k was 0.227. A section of the coating from the coated panel portion outside the PMMA cylinder was removed to the bare substrate. This bare steel section was used as the working electrode and was connected to one end of a potential-applied source. The other end of the potential-applied source was connected to the copper wire attached to the steel disk. A battery and a potentiostat were tested as sources to apply the potential difference between the scribe (defect) and the glass tube (blister). However, for an unknown reason, the potentiostat interfered with both the pH and the Na ion concentration readings. For that reason, the potential source employed in this experiment consisted of two 1.5 V batteries in series connected in series with a variable resistor. This arrangement provided a current of 45 ± 5 μA and a corresponding potential of 275 ± 45 mV.

4.2 Cation Measurement

The experimental apparatus for cation measurement in the glass tube is depicted schematically in figure 5 and shown in the photograph in figure 6. The concentration of Na ions in the glass tube was measured by a commercial 1 mm tip, Na-selective

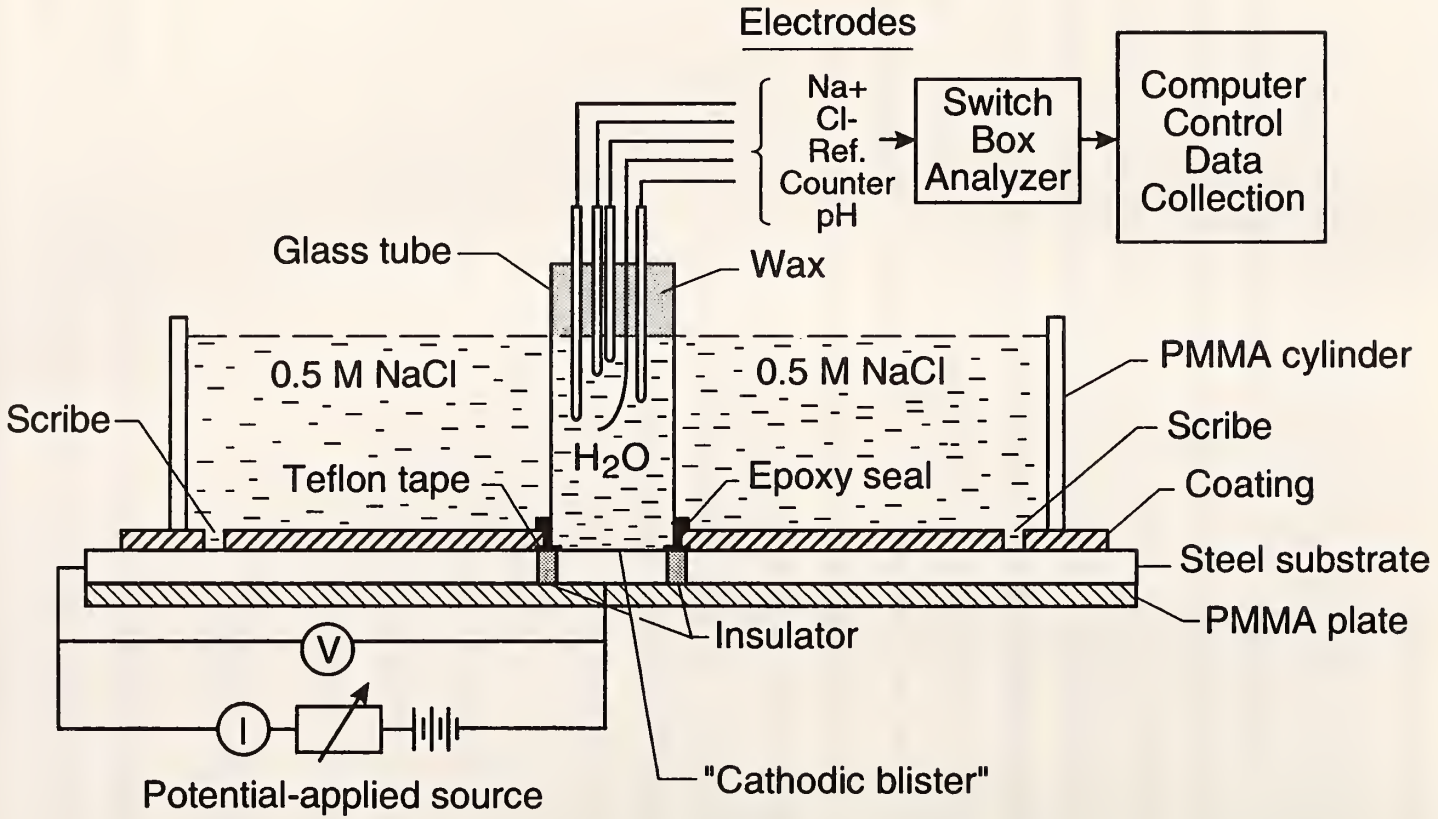

Figure 5. Schematic of Experimental Apparatus and Specimen Configuration .

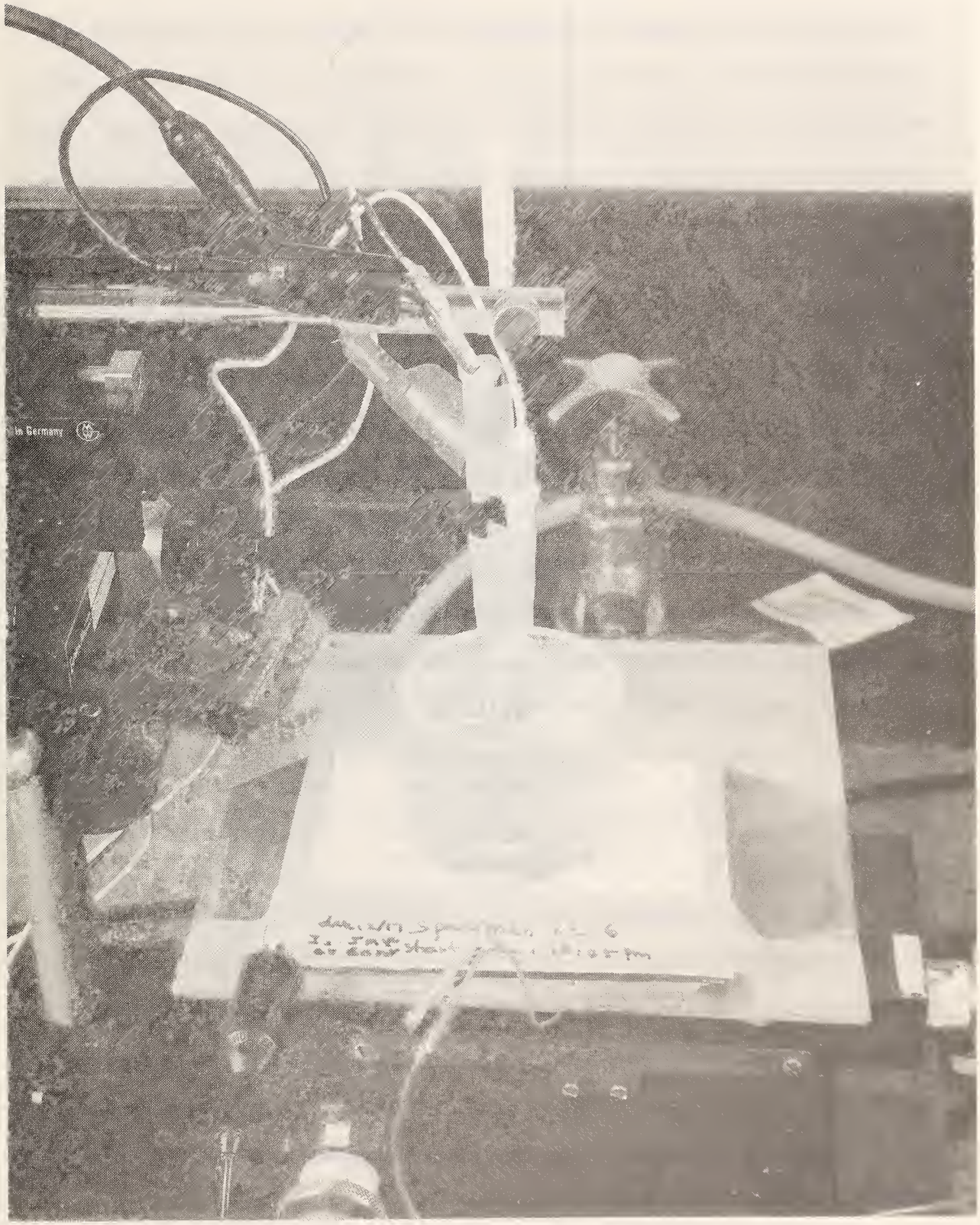

Figure 6. Experimental Apparatus for Cation Measurement .

minielectrode (World Precision Instruments*). In addition, the pH in the glass tube was determined as a function of time by a conventional mini pH electrode. A 10x10 mm platinum foil attached to a silver wire was used as the counter–electrode. The electrodes were connected to a high–impedance (10^{14} ohm) pH/ion analyzer (Orion EA 940•). The analyzer was programmed to record Na ion concentrations and pH at desired intervals. The ion–selective electrodes respond to activity rather than concentration, where the activity is related to the concentration by the activity coefficient. However, because the measurement system was calibrated in terms of concentration, we reported our results in terms of concentration. A switch box was employed to provide simultaneous readings of multiple electrodes. Both pH and Na–selective electrodes were calibrated prior to actual measurements using standard solutions. Before measurements began, a 0.5 mol/L solution of reagent grade NaCl in doubly distilled, deionized water was placed in the space between the glass tube and the PMMA cylinder, and doubly distilled, deionized water was added to the inside of the glass tube. The liquid in the glass tube and in the PMMA cylinder were always kept at the same level, about 4 mm from the rim. The top end of the glass tube was sealed with molten paraffin wax and cellophane was used to cover the top of the PMMA cylinder. These procedures were employed to minimize evaporation of water from both containers. Two pointed micropipettes were inserted through the wax. One was used to introduce air into the glass tube at a rate of approximately 10 bubbles per minute to maintain the corrosion reactions. This micropipette was also used to add NaCl solution into the glass tube to maintain the original liquid level. This provides justification for the model assumption of constant blister volume. The other micropipette was used to release the pressure. To facilitate the handing of the measurement system, both the specimen and the electrodes were attached to separate micromanipulators.

5. Results and Discussion

5.1 Experimental Results

Figure 7 shows the pH and Na ion concentrations in the central chamber (control glass tube) as a function of time. The data on which the figure is based are given in Appendix I. The concentration of Na ion in the glass tube started to increase after more than 280 hours of testing, and surpassed the concentration in the PMMA cylinder around 450 h. The pH in the glass tube also started to increase at about 280 h and reached a value of almost 11 after 430 h; after that it remained essentially unchanged. It should be noted that approximately 2 μl of solution with the same Na ion concentration as that in the glass tube was added to the glass tube at a time of 650 h in order to restore the original liquid level. This may have disturbed the corrosion reactions as well as the sodium ion transport process, which may help to explain the apparently anomalous value of Na ion concentration at 720 h exposure.

The bare steel substrate inside the glass tube did not corrode and remained "white." The high pH solution and the whiteness of the steel area inside the tube indicate that this area was in the cathodic state during the experiment. On the other hand, the steel substrate at the scribe became heavily corroded, indicating that these regions were anodic. These results suggest that the experiment was successful in simulating the blister formations and delamination processes generally observed around defects of coated steel panels exposed to electrolytes. The defects serve as the anode where iron oxidizes (corrodes), and the delamination and blister areas serve as the cathode where hydroxide ions are formed. Under coatings, pH values as high as 14 have been measured in cathodic regions [13]. Because of these processes, an induced potential develops and current flows between the anode and cathode.

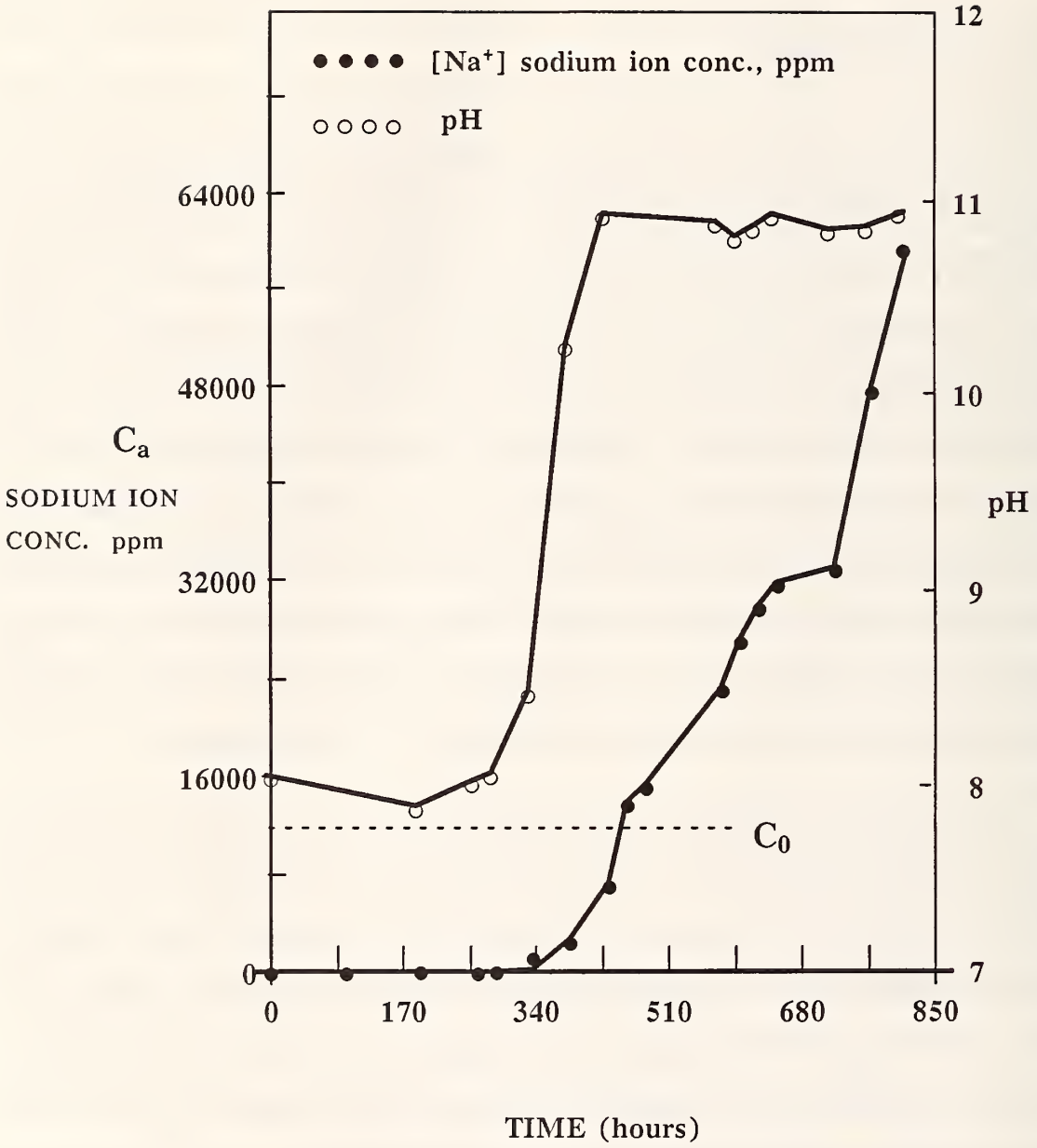

Figure 7. Sodium Ion Concentration and pH within Central Glass Chamber .

It is interesting to note that the results of the same experiment conducted for 600 h but in the absence of an applied potential difference between the scribe and the glass tube showed that: 1) the bare metal in the glass tube and at the scribe corroded severely, 2) the concentration of sodium ion inside the glass tube varied very little between the start and the end of the experiment (between 3 and 7 ppm), and 3) the pH in the glass tube decreased, from 8.2 at the beginning to 7.7 at the end of the exposure. These results indicated that, in the absence of an applied potential, the bare metal inside the glass tube was in the anodic state, and not in the cathodic state as in the potential–applied case. The cathodes probably remained somewhere under the coating in these experiments.

5.2 Theoretical Results

In this section theoretical results are presented based on the mathematical models developed in section 3. The computer programs used to implement the calculations are given in Appendix III.

5.2.1. Steady State Sodium Ion Concentration

From the previous mathematical analysis, it is clear that, between the scribe and the blister on a coating/metal interface, two major parameters affect the sodium ion steady state concentration profile. One parameter is the geometric factor k (aspect ratio). The other is the parameter p, which is a measure of the relative importance of the applied electric field as opposed to diffusion as an ionic transport mechanism. Since these two mechanisms occur in parallel, the faster one will control transport. Thus, at low values of p, diffusion controls transport while, at high values of p, transport of ions is controlled by the potential gradient created by the electric field. Our

experimental results suggest that transport is controlled by the electric field when a potential is applied across the system.

Figure 8 (plotted from eq (8)) presents the sodium ion steady state concentration profile with k as a parameter and no potential gradient ($p = 0$). The value $k = 0.227$ corresponds to that for the size of blister employed in our experiment. High sodium ion concentrations are present close to the scribe and decrease along the path from the scribe to the blister. The concentration gradients, which are proportional to the slopes of the curves, are lower near the scribe where the ions first enter the channel under the coating. The x–intercept ($k/(1-k)$) corresponds to the blister radius ($r = a$). The concentration is zero there, as indicated by eq (8).

Figures 9, 10, and 11 (plotted from eq (12)) display the steady state sodium ion concentration profile with p as a parameter at different values of k. The figures show that the sodium ion concentration decreases faster at greater values of p near the blister, but slower near the scribe, an effect that is accentuated for smaller blisters, as shown in figure 11. Comparing these three figures shows that, when p is constant, the gradients of sodium ion concentration profile are smaller at larger values of k. Higher potential gradients along the path from the scribe to the blister lead to both higher ion concentrations in the region near the blister and higher gradients. This effect is expected since higher values of p result in facilitated ion diffusion under the coating.

5.2.2. Steady State Ion Flux

Figure 12 (plotted according to eqs (10) and (11)) displays the steady state dimensionless sodium ion flux plotted against the reciprocal of the aspect ratio 1/k, with p given as a parameter. The flux is negative because sodium ions are moving inward in the direction of decreasing radius.

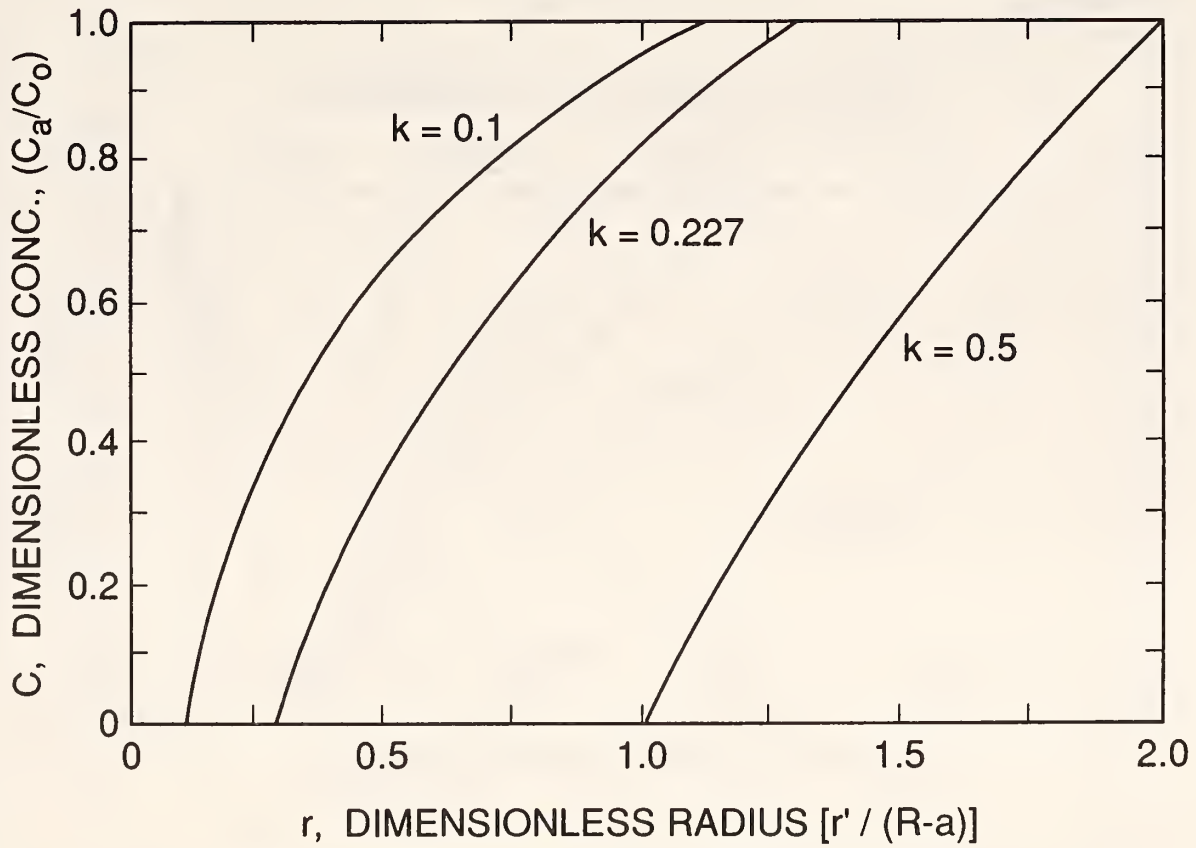

Figure 8. Steady State Sodium Ion Concentration Profile: C vs. r.

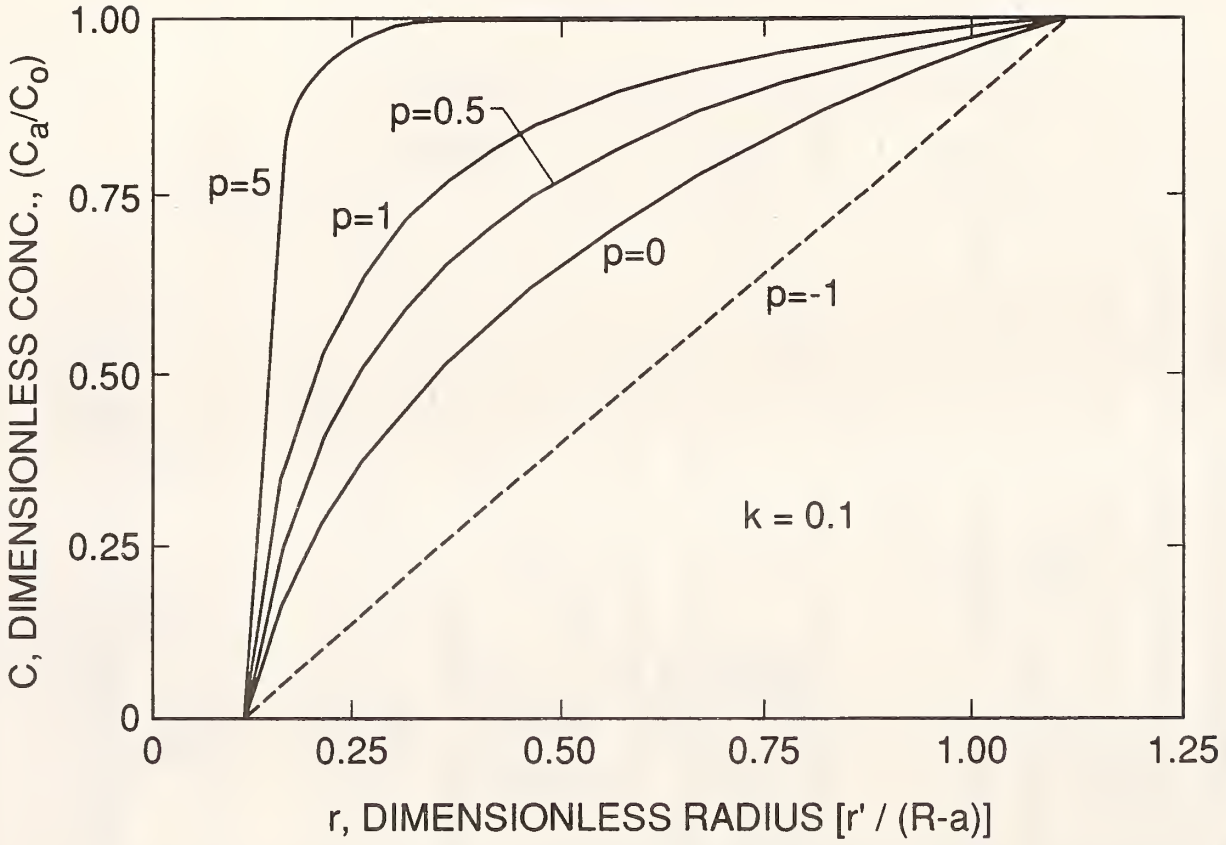

Figure 9. Steady State Sodium Ion Concentration Profile: C vs. r (with k = 0.1) .

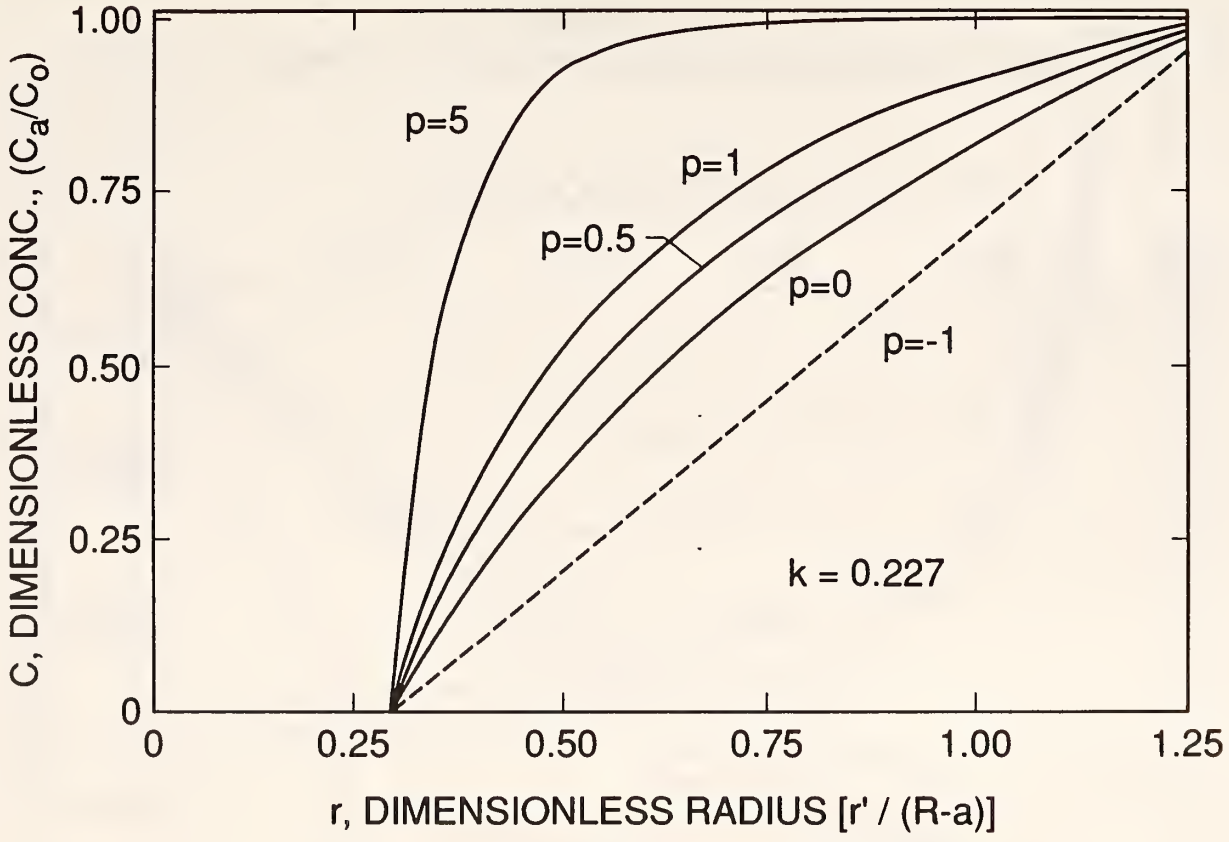

Figure 10. Steady State Sodium Ion Concentration Profile: C vs. r (with k = 0.227).

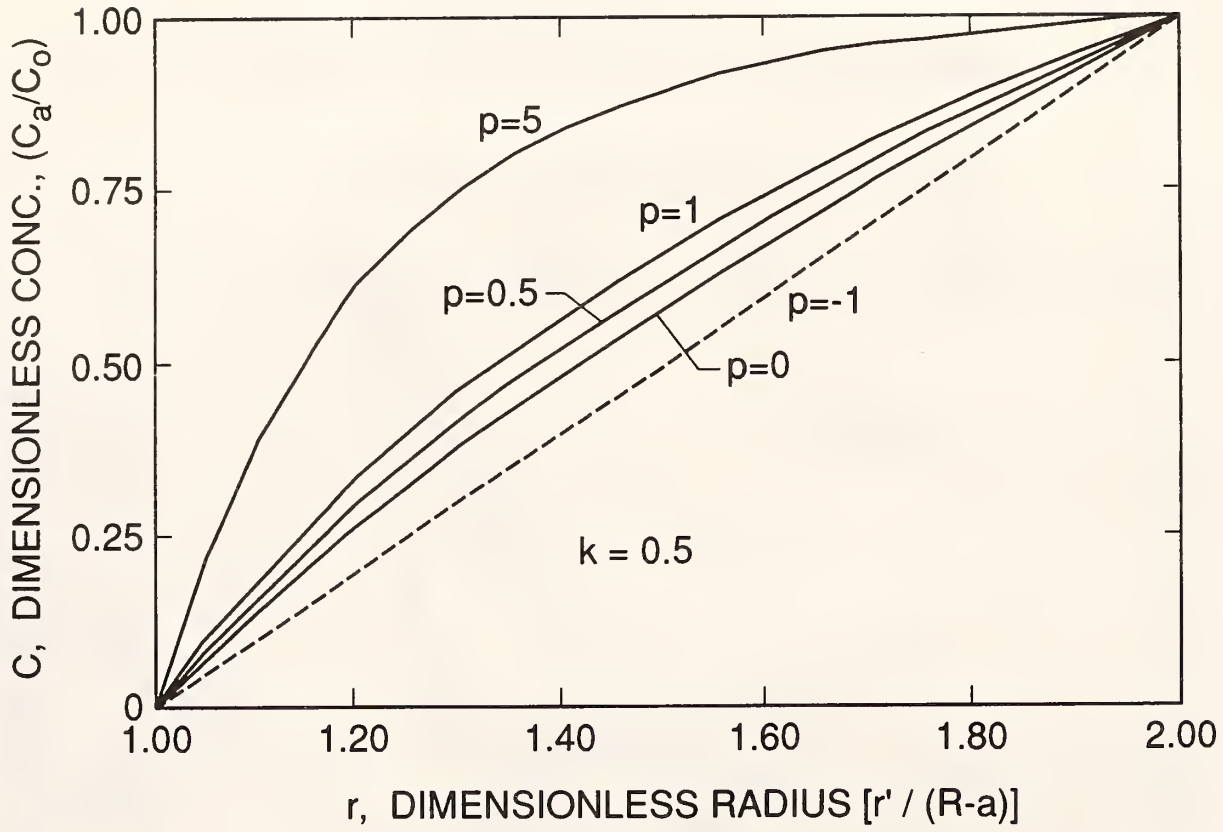

Figure 11. Steady State Sodium Ion Concentration Profile: C vs. r (with k = 0.5).

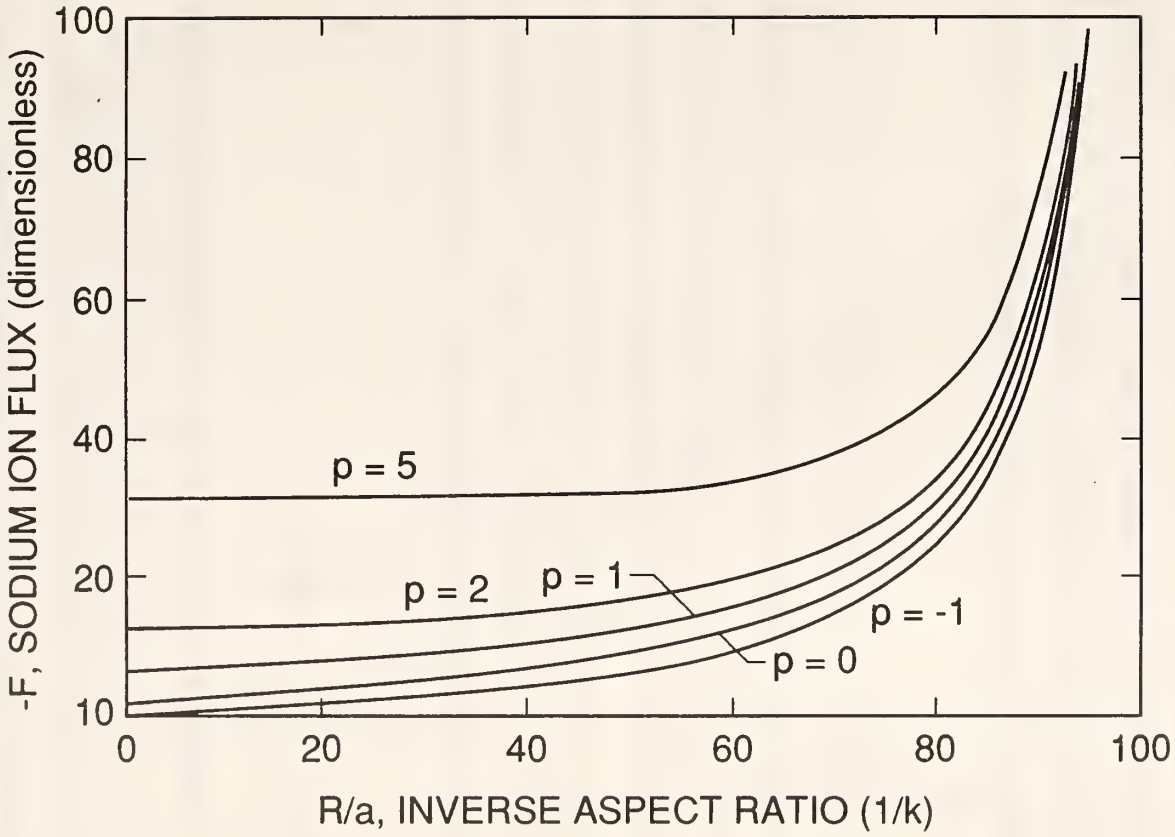

Figure 12. Steady State Sodium Ion Flux, (-F) vs. k.

As shown in figure 12, the ion flux is much higher when the scribe and blister are near one another (when R/a is larger) and decreases rapidly as their distance of separation increases, approaching a constant flux for smaller blisters.. For constant k values, when p is larger, the ion flux is greater. For example, the flux when $k = 0.1$ ($R = 10a$) is 2.5 times as high with $p = 1$ as it is with no electric field ($p = 0$). This illustrates that a higher potential gradient causes a higher ion flux. These steady state results for the ion flux agree with the long time unsteady state predictions of Nguyen *et al* [12] and tend to lend validity to the accuracy of both the formulation and numerical solution they employed.

Figure 13 shows how the predicted dimensionless ion flux F changes with parameter p with k as a parameter. As is also apparent in figure 12, F increases when p does. For the same p, F also increases when k increases, but the effect is not as dramatic at larger values of p. For p values larger than about 6, the flux becomes independent of k when $k < 0.5$. This fact shows that when p exceeds a certain value, different blister sizes will not affect the steady state ion flux in the path between the blister and the scribe. Of course, larger blisters will still garner more sodium ions because of their increased size.

5.2.3. Critical Value of Parameter Value p

In the previous section, the critical value of the dimensionless potential gradient p^* was defined as $p^* = (1-k)/k \ln(1/k)$. From the experimental data given in table 1, $k = 0.227$, giving $p^* = 2.295$. As discussed earlier, when $p \geq p^*$ (p value above or equal to the critical value), there will be no steady state concentration of sodium ion within the blister, and the final concentration is predicted to increase indefinitely.

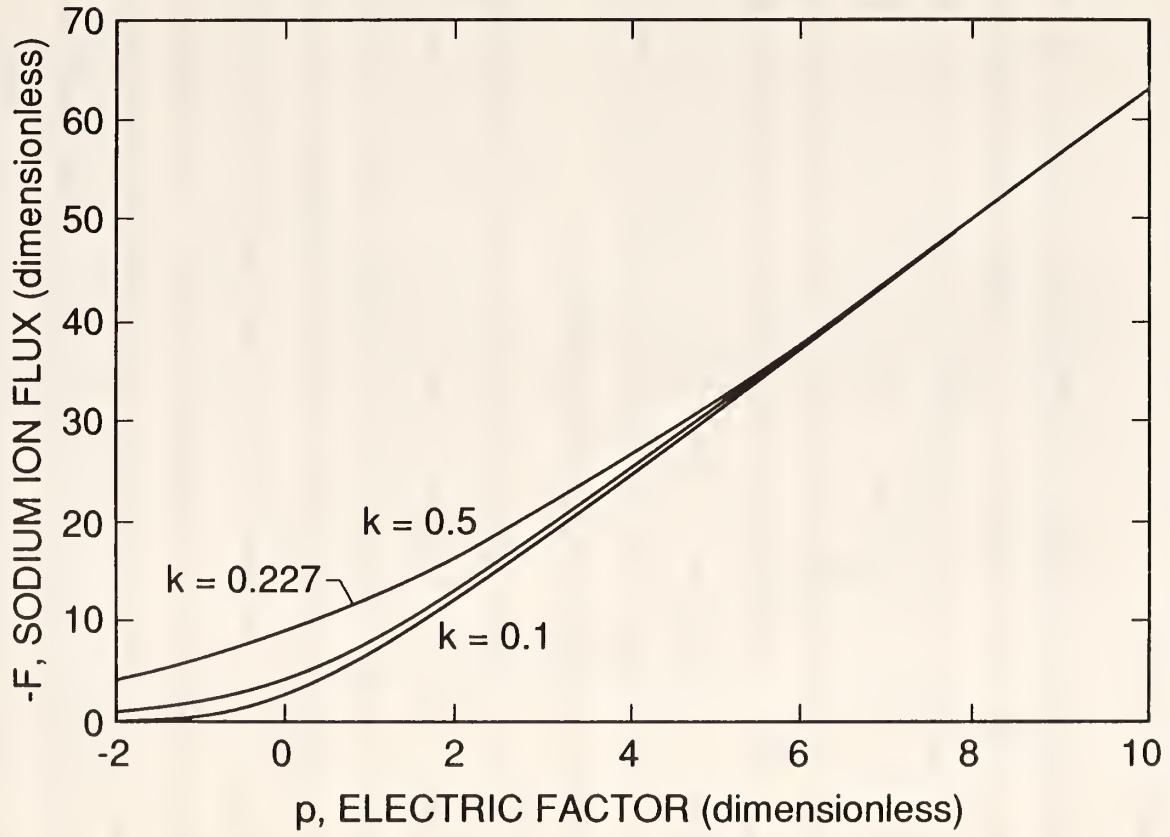

Figure 13. Steady State Sodium Ion Flux, (-F) vs. p.

When $p = 0$, the steady state concentration within the blister will reach the value in the outside solution, while when $p < p^*$ a steady state concentration of sodium ion will be reached within the blister. If p is negative the final concentration of ions is predicted to be less than the external value C_0. In this event the electrical field opposes the inward diffusive flow of ions.

Figure 14 (plotted using eq (31)) shows how the steady state sodium ion concentration in the blister varies with the ratio of p to p^*. When p is less than half of the critical value p^*, the concentration increases slowly as p increases. However when p is greater than this, the concentration rises rapidly becoming unbounded as p approaches p^* from below. The figure shows that when $p = 0$ the steady state concentration becomes equal to that in the external solution, while for p values greater than p^* there is no steady state concentration. As shown by the dashed part of the curve, if negative values of p were possible they would produce somewhat lower steady state concentrations. These results agree with model predictions.

Figure 15 presents the steady state sodium ion concentration within the blister versus k (in the range from 0 to 0.9) with p as parameter (for $p = -1$ to 5). Small values of k correspond to the situation where the size of the blister is small compared with the distance between the blister and the scribe, while high k corresponds to a relatively large blister. The figure shows that when $p > 0$, the steady state concentration exceeds the external solution concentration. Concentrations within larger blisters are predicted to be greater than within smaller blisters, the effect being more pronounced at larger values of p. When $p = 0$, the final concentration within the blister is predicted to be equal to that in the external solution regardless of blister size. Negative values of p predict that concentrations within the blisters will be less than the external value with larger blisters being more dilute than smaller. This is unlikely in practice, since

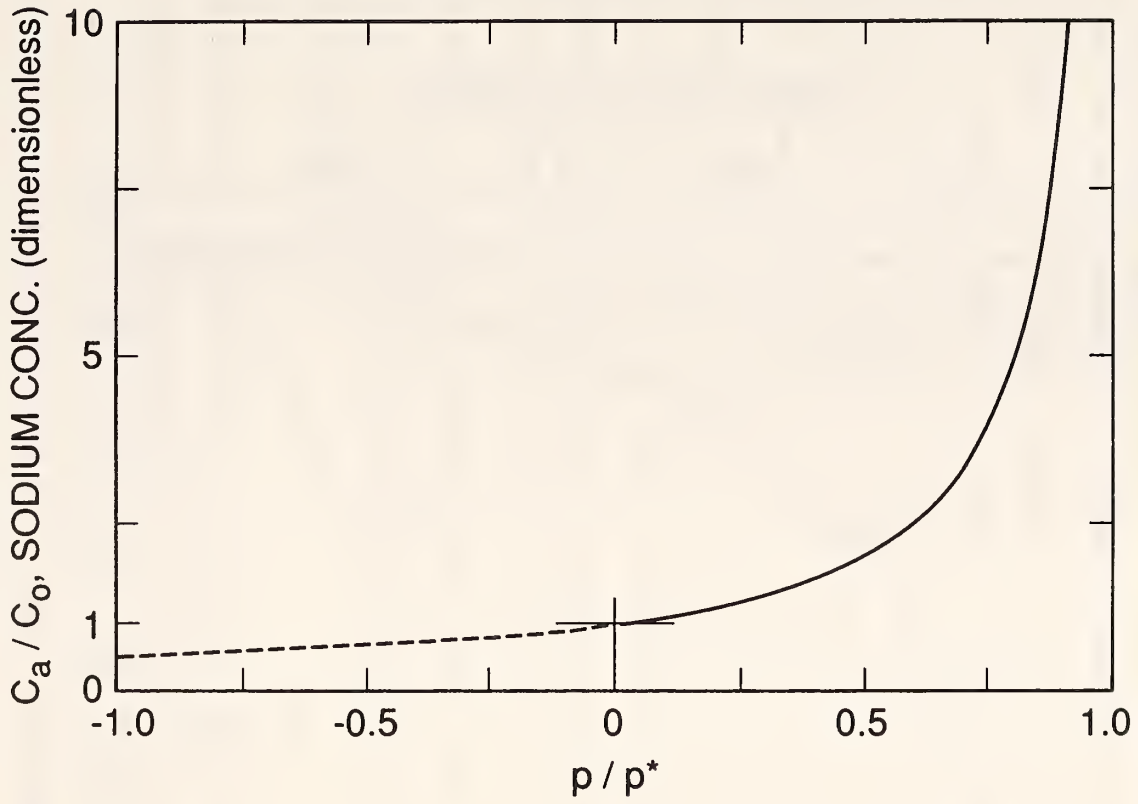

Figure 14. Steady State Sodium Ion Concentration, C_A/C_0 vs. p/p^*.

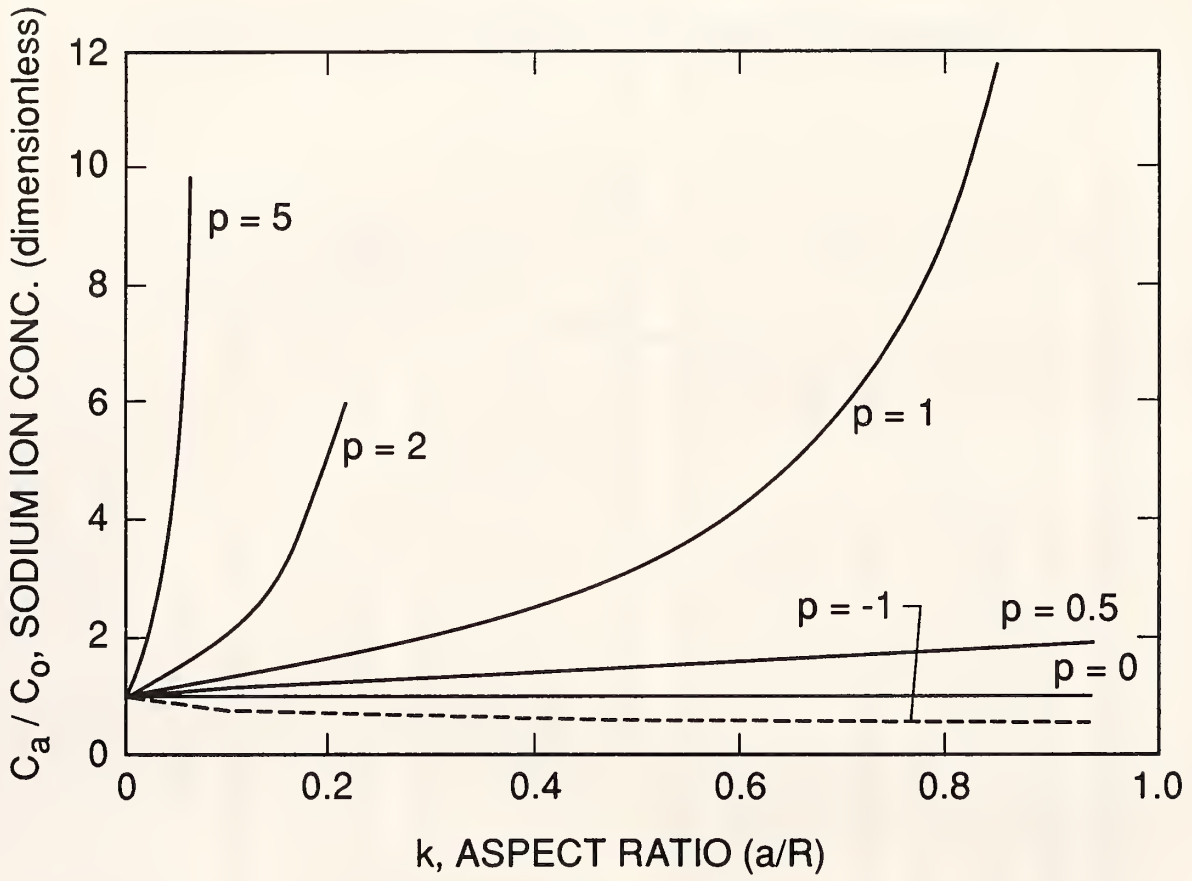

Figure 15. Steady State Sodium Ion Concentration, C_A/C_0 vs. k.

as mentioned, the corrosion reactions cannot be sustained at their original site when the polarity of the scribe and blister are reversed.

Figure 16 displays the way the critical value p^* changes with k, the ratio of a to R. The experimental values ($p^* = 2.29$ at $k = 0.227$) are marked on the figure for reference. When $k < 0.1$, p^* decreases rapidly with increases in k, while for k values above 0.1, p^* is not as sensitive to variations in k. Figure 16 shows that for larger blisters (larger a for the same R) p^* is near unity, whereas for small ones, p^* can be quite large. Since $p < p^*$ is the criterion for obtaining a steady state concentration within a blister, it is less likely that large blisters will develop a steady state concentration of salt within them. Once the blisters reach a critical size corresponding to $p = p^*$ they may continue to grow. If such a blister enlarges due to the osmosis or cathodic delamination induced by the increased salt concentration within it, p^* will fall even further (provided the scribe location is fixed). The new larger blister will have more of a tendency to grow because the higher salt concentration within it will lead to an even higher osmotic pressure. The larger surface area of the larger blister will also draw in more salt than that in the smaller blister. The high pH within the blister can also lead to delamination (cathodic) around the periphery of the blister. These factors can cause the eventual failure of the coating system.

Small or nascent blisters are predicted to be less prone to grow than large ones. This may supply part of the reason for the induction period often observed with blister growth. The initial or breakthrough time Θ_i provides an alternative explanation, as does the initial unsteady state period.

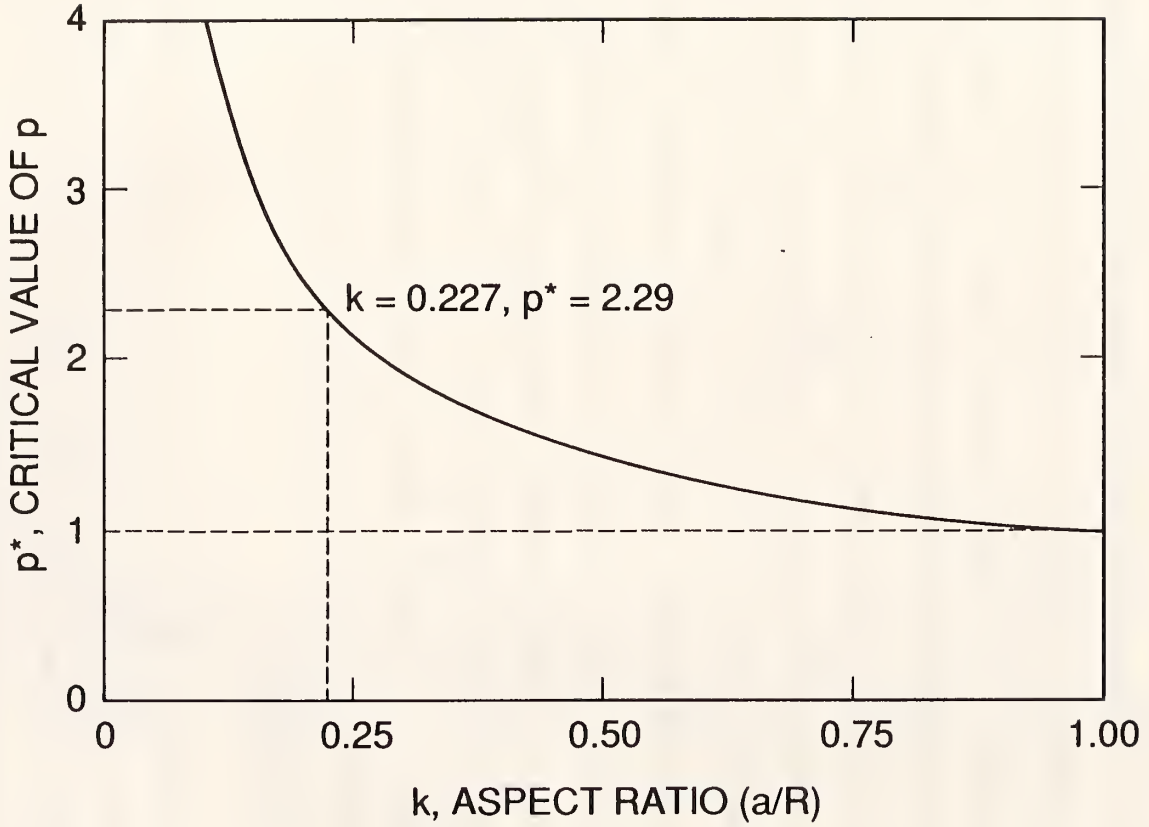

Figure 16. Critical Value of p* vs. k .

5.3 Comparison of Experimental to Theoretical Results

Since the sodium ion concentration does not begin to rise from background levels until almost 280 hours, the initial stage will be of comparable duration. It takes about this long for the sodium ions to break through into the blister. The initial stage will end and the propagation stage will begin at this time ($t = \Theta_i$).

Equation (31) predicts how the sodium ion concentration varies with time. In this equation, there are two unknown constants, α and β, which are defined in terms of the parameters p, k, V, D, and δ. However, there is not enough information to determine all of these parameters individually. The experimental data presented in Appendix I as table 1 were used to find the best values of α and β. The data analysis algorithm is presented in Appendix II while the computer codes for this calculation are given in Appendix III. The best values of α and β are the ones which minimize the error sum of squares between the predicted and the experimental concentration data.

A Fortran program (refer to FINDAB program in Appendix III) was coded to employ the curve–fitting method and obtain the best values of α and β. The experimental data of table 1 show that breakthrough of sodium ion into the blister appears to occur some time between 264 and 288 h, with a definite breakthrough observed by 336 h. Thus, the initiation times $\Theta_i = 264$ and 288 h were used to perform the data analysis. This resulted in values for (α, β) pairs of (–0.4627, 4.48E–03 hr^{-1}) and (–0.465, 4.84E–03 hr^{-1}), respectively. A nonlinear least square computer program [14] using the same data set was also employed. It gave equivalent (α, β) pairs for the same initiation times. The consistency of the results lends credence to the methods employed in the data analysis. A somewhat lower error sum of squares was obtained

with $\Theta_i = 264$ hours, but the variance ratio (F) test showed that it was not statistically better than the value for $\Theta_i = 288$ h.

Figures 17 displays both the theoretical and experimental data of sodium ion concentration versus time within the blister for the two initiation times. The best value of p was 3.35 for both breakthrough times. Note that the curves are both curved upward and nearly coincident. The upward curvature shows that the concentration is increasing without limit. Since $p > p^* = 2.29$, the theory predicts that a steady state concentration will not be reached within the blister. In fact, at the conclusion of the experiment, the concentration of sodium ions within the blister was over five–fold that in the external solution. The concentration is predicted to increase without bound as long as there are sufficient sodium ions in the external solution. If the simulated blister modeled by the experiment were an actual blister under a coating there is a good chance that it would keep enlarging for the reasons previously discussed. Further experimental and theoretical work is currently being directed in our laboratories towards an understanding of the mechanisms and modes of blister growth.

Although separate values of the diffusion coefficient D and channel height δ can not be found, their product $D\delta$ can be calculated from the lumped parameter β. From the best values of β the product $D\delta$ is 0.92 E–6 and 0.97 E–6 cm^3/s, for initiation times of 264 and 288 h, respectively. For a channel height of 1 mm the values of D are approximately 1 E–5 cm^2/s, which is somewhat lower than the value of the unhindered or bulk diffusivity of 1.5 E–5 cm^2/s for sodium chloride [15].

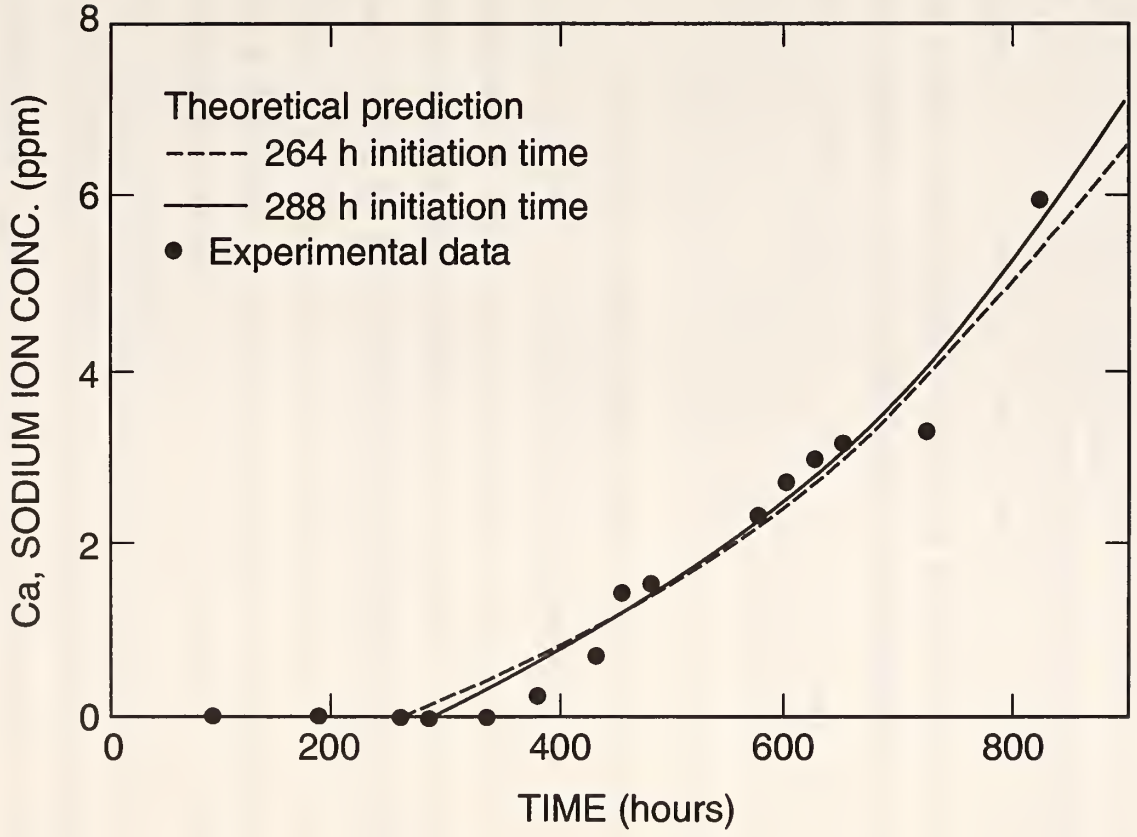

Figure 17. Sodium Ion Concentration within Blister vs. Time .

6. Summary and Conclusions

Conceptual and mathematical models have been developed for blistering of organic coatings on metal substrates that results from corrosion when defects are present in the coating and the coated metal is exposed to electrolytic solutions. Experiments were conducted in a cylindrical geometry which simulated this situation. Sodium ions in an outside chamber containing an external scribe or defect which acted as an anode were transported under the combined influence of diffusion and potential gradients towards an inner chamber which served the role of a cathodic blister. Solutions to the model predicted that the steady state sodium ion concentration profile, and the sodium flux in the region between the blister and the scribe, should be a function of the dimensionless potential gradient p and aspect ratio k. These predictions are consistent with the long time unsteady state results of the work of Nguyen *et al* [12].

An unsteady state solution was developed for the concentration of sodium ion within the blister as a function of time. In the absence of an electric field ($p = 0$) the highest ion concentration that can exist within a blister is that in the external solution. Under the application of a cathodic potential ($p > 0$), the concentration within the blister is predicted to rise above that in the external solution. A critical value p^* of the dimensionless potential gradient, which is solely a function of the aspect ratio, established the conditions under which the concentration would reach a steady value ($p < p^*$) or increase indefinitely ($p \geq p^*$). The model was successfully fitted to experimental data which did show $p > p^*$. For blisters that are changing size, the theory predicts that small blisters will not grow until they reach a critical size corresponding to ($p = p^*$). Blisters of larger size can grow under the combined effects of cation transport, osmosis, cathodic delamination and mechanical stresses.

The results of this study should be of general applicability to other similar coating and electrolyte systems.

7. Nomenclature

a radius of the blister.

a' constant defined by eq (20).

C_0 sodium ion concentration outside the scribe (or defect).

C_a sodium ion concentration within blister.

C' sodium ion concentration between the scribe and the blister for the initial period.

C dimensionless concentration of sodium ion, $C = C'/C_0$.

D effective diffusion coefficient of sodium ion under coating.

E strength of electric field.

F dimensionless ion flux between the scribe and the blister.

F_e ion flux into blister caused by electric field.

H height of the blister.

k geometric aspect ratio for the blister, a/R.

k_i geometric aspect ratio for the moving interface, $k_i = r_i/R$

L length scale

p dimensionless potential gradient.

p* critical value of the dimensionless potential gradient, (k–1)/(k lnK)

R radius of the scribe.

r' radial coordinate.

r dimensionless radius.

r_i radius of the moving interface.

t dimensionless exposure time.

t' exposure time.

V volume of solution in blister

w_d molar flow caused by diffusion.

w_e molar flow caused by the electric field or potential gradient.

α constant defined by eq (32), $1-p/p^*$.

β constant defined by eq (33)

$\bar{\varrho}_s$ amount of adsorbed sodium per unit of interfacial area.

δ channel height.

μ average mobility of sodium ion.

Θ_i initiation or breakthrough time for the sodium ion.

$\Delta\Phi$ potential difference between scribe and blister.

8. References

[1.] Bennett, L. H., Kruger, J., Parker, R. L., Passaglia, E., and Yakowitz, H., Natl. Bur. Stand., U.S. Spec. Publ. 511–1, 1978.

[2.] Pommersheim, J. M., Campbell, P. and Mcknight, M., "The Mathematical Modeling of the Corrosion Protective Performance of Organic Coatings," Nat. Bur. of Stand. U.S. Technical Note 1150, September 1982.

[3.] Leidheiser, H. Jr., J. Adhesion Sci. Technol., 1 (1987) 79.

[4.] Koehler, E. L., Corrosion, 40 (1984) 5.

[5.] Watts, J. W., J. Adhesion, 31 (1989) 73.

[6.] Funke, W., Leidheiser, H. Jr., Dickie, R.A., et. al., *J. Coatings Technology, 58 (1986) 741*

[7.] Walter, G. W., *Corrosion Sci., 26* (1986) 27.

[8.] Nguyen, T., Byrd, E., and Lin, C., J. Adhesion Sci. Technol., 9 (1991) 697.

[9.] Beaunier, L., Epelboin, I., Lectrade, J. C., and Takenouti, Surface. Technol., 4 (1976) 237.

[10.] Funke, W., Ind. Eng. Chem. Prod. Res. Dev., 24 (1985) 343.

[11.] Sato, N., Corrosion, 45 (1989) 354.

[12.] Nguyen, T., Hubbard, J.B., and McFadden, G.B., *J. Coatings Technol*, 63 (1991) 43.

[13.] Ritter, J. J. and Kruger, J., in Corrosion Control by Organic Cratings, Leidheiser, H. Jr. (Ed.), Natl. Assoc. Corros. Eng., Houston, TX, 1981, p. 28.

[14.] Koko, F. W., BUST (Bucknell University Statistics Program).

[15.] Robinson, R. A., and Stokes, R. H., "Electrolyte Solutions," 2nd ed., Academic Press, New York (1959).

Appendices

I. Experimental Data

II. Data Analysis

III. Computer Codes

Appendix I. Experimental Data

Table 1: Experimental Data

1. *Data for Blister Size*

Radius of blister: $a = 0.5$ cm

Radius of scribe: $R = 2.2$ cm

Height of blister: $H = 4$ cm

Volume of blister: $V = \pi a^2 H = 3.14\ cm^3$

2. *Data for Concentrations (ppm) of Sodium Ion within Blister*

$C_0 = 11500$ ppm

Time (hours)	C_A ($[Na^+]$, ppm)	pH
0	3.3	8.05
96	3.7	.....
192	3.4	7.89
264	3.7	8.02
288	45	8.06
336	250	8.48
384	2640	10.25
432	7300	10.93
456	14020	.....
480	15500	.....
576	23300	10.89
600	27200	10.82
624	29900	10.87
648	31900	10.93
720	33110	10.85
768	47610	10.87
816	59420	10.95

Appendix II. Data Analysis

The curve fitting method developed here was used to analyze the experimental data of the sodium ion concentration within the blister versus time.

Equation (31) was used to evaluate the best values of the model constant α and β. The experimental data is given in table 1.

$$\frac{C_A}{C_0} = \frac{1}{a}\left[1 - e^{-a\beta(t-\Theta_i)}\right], \qquad For\ a \neq 0, \tag{31}$$

$$\text{where } a = 1 - p\frac{k\ln(1/k)}{1-k} \tag{32}$$

$$\text{and } \beta = \frac{2\pi\ \delta\ D}{V\ln(1/k)}\ . \tag{33}$$

In this method the error sum of squares s^2 is minimized, where:

$$s^2\ (\ a,\ \beta\ ) = \sum(\ y_i - y_c\ )^2$$

and s is the variation ($y_i - y_c$), where y_i is the experimental value, and y_c is the value calculated from the model equations and assumed model constants.

The algorithm used to evaluate the best values of α and β is as follows:

1. Pick a value of β;
2. Pick a value of α;
3. Apply the values of α and β to eq (31) or eq (37);
4. Plot s^2 versus β at different α's. Find the lowest value of s^2.
5. Pick a new value of β and repeat steps 2 to 4.
6. Finally find the global minimum value of s^2, and the associated best values of α and β.

Appendix III. Computer Codes

1. Program SSCONC
2. Program SSFLUX1
3. Program SSFLUX2
4. Program CVSKP
5. Program CCPP
6. Program PK
7. Program FINDAB
8. Program NEWDATA

```
      PROGRAM  SSCONC
C
C
C   ***************************************************************
C   *                                                             *
C   *    TITLE:                  Steady-State Concentration Profile   *
C   *                                                             *
C   *    AUTHOR:                 Joanne Zhang                     *
C   *                                                             *
C   *    DATE Coded:             February  17, 1990               *
C   *                                                             *
C   *    ORGANIZATION:           Chemical Engineering Department  *
C   *    LOCATION:               Bucknell University              *
C   *                            Lewisburg, PA   17837            *
C   *                                                             *
C   ***************************************************************
C
C
C:    PURPOSE:
C     -------
C
C          This program calculates the steady-state ion concentration
C       profile along the channel beneath coating films with potential
C       gradient p and aspect ratio k as parameters.
C
C
C:    VARIABLES:
C     ----------
C
      REAL       C, R
      REAL       R0, RT, DR
      REAL       P, K
      REAL       CON(20), RI(20)
C
C
C:    INITIALIZATION:
C     --------------
C


C
C
C   ++++++++++++++++++++++++++++++++++++++++++++++++++++++++++++++++
C
C:    BODY:
C     ----
C
C:       Data Input
C
      PRINT*, 'PLEASE INPUT THE VALUES OF K:'
      READ*, K
C
      PRINT*, 'PLEASE INPUT THE VALUES OF P:'
      READ*, P
C
C:       Calculate R0 (r=a) and RT (r=R)
C
      R0 = K/(1-K)
      RT = 1/(1-K)
C
C:       Calculate concentration
C
      DR = (RT - R0)/20.
      R = R0
C
      DO 10  I = 1, 20
         IF (P .EQ. 0.0) THEN
            C = 1/LOG(1/K)*LOG(R/R0)
         ELSE
            C = 1/(K**P-1)*(R0**P/R**P-1)
         ENDIF
```

```
         CON(I) = C
         RI(I)  = R
         R = R + DR
   10  CONTINUE
C
C:       Data output
C
      OPEN (UNIT = 9, FILE = 'f2b.5')
C
      DO 20  J = 1, 20
         WRITE(*, 55)     RI(J), CON(J)
         WRITE(9, 55)  RI(J), CON(J)
   20  CONTINUE
C
C
C:    TERMINATION:
C     -----------
C
   55  FORMAT(1X, F7.4, 3X, F7.5)
C
      END
```

```
      PROGRAM  SSFLUX1
C
C
C   ********************************************************************
C   *                                                                  *
C   *    TITLE:                   Steady-State Flux vs. K              *
C   *                                                                  *
C   *    AUTHOR:                  Joanne Zhang                         *
C   *                                                                  *
C   *    DATE Coded:              March  16, 1991                      *
C   *                                                                  *
C   *    ORGANIZATION:            Chemical Engineering Department      *
C   *    LOCATION:                Bucknell University                  *
C   *                             Lewisburg, PA   17837                *
C   *                                                                  *
C   ********************************************************************
C
C
C:    PURPOSE:
C     -------
C
C          This program calculates the steady-state ion flux along
C       the channel beneath the coating films.  The flux varies with
C       aspect ratio k with potential gradient p as a parameter.
C
C
C:    CONSTANTS:
C     ---------
C
      REAL       PI
      PARAMETER  (PI = 3.14)
C
C
C:    VARIABLES:
C     ---------
C
      REAL       F(99), K(99)
      REAL       P
      REAL       KI
C
C
C:    INITIALIZATION:
C     --------------
C

C
C
C   ++++++++++++++++++++++++++++++++++++++++++++++++++++++++++++++++++++
C
C:    BODY:
C     ----
C
C:       Input value of P.
C
      PRINT*, 'Input value of P: '
      READ*, P
C
C:       Calculate F as a function of K.
C
      PRINT*, ' K          F'
      KI = 0.01
C

      IF (P .EQ. 0.0) THEN
         DO  10  I = 1, 99
            K(I) = I*KI
            F(I) = ABS(2*PI/LOG(K(I)))
            WRITE(*, 55) K(I), F(I)
 10      CONTINUE
```

```
      ELSE
         DO 20   I = 1, 99
            K(I) = I*KI
            F(I) = ABS(2*PI*P/(K(I)**P - 1))
            WRITE(*, 55) K(I), F(I)
 20      CONTINUE
      ENDIF
C
C:       Data output.
C
      OPEN (UNIT=9, FILE = 'f3.-1')
C
      DO  30  J = 1, 99
        WRITE(9, 55)  K(J), F(J)
 30   CONTINUE
C
C
C:    TERMINATION:
C     -----------
C
 55   FORMAT (F6.3, 1X, F10.6)
C
      END
```

```
      PROGRAM  SSFLUX2
C
C
C   ********************************************************************
C   *                                                                  *
C   *    TITLE:                  Steady_State Flux vs. P               *
C   *                                                                  *
C   *    AUTHOR:                 Joanne Zhang                          *
C   *                                                                  *
C   *    DATE Coded:             March  17, 1991                       *
C   *                                                                  *
C   *    ORGANIZATION:           Chemical Engineering Department       *
C   *    LOCATION:               Bucknell University                   *
C   *                            Lewisburg, PA   17837                 *
C   *                                                                  *
C   ********************************************************************
C
C
C:    PURPOSE:
C     -------
C
C          This program calculates the steady-state ion flux along
C       the channel beneath the coating films.  The flux varies with
C       potential gradient p with aspect ratio k as a parameter.
C
C
C:    CONSTANTS:
C     ---------
C
      REAL       PI
      PARAMETER  (PI = 3.14)
C
C
C:    VARIABLES:
C     ---------
C
      REAL       F(25), P(25)
      REAL       K
C
C
C:    INITIALIZATION:
C     --------------
C

C
C
C   ++++++++++++++++++++++++++++++++++++++++++++++++++++++++++++++++++++
C
C:    BODY:
C     ----
C
C
C:       Input value of k.
C
      PRINT*, 'Input value of K: '
      READ*, K
C
C:       Calculate F as a function of P.
C
      PRINT*,
      PRINT*, ' P          F'
      P(1) = -2.0
C
      DO  10  I = 1, 25
         P(I) = P(1) + (I-1)*0.5
         IF (P(I) .EQ. 0.0) THEN
            F(I) = ABS(2*PI/LOG(K))
         ELSE
            F(I) = ABS(2*PI*P(I)/(K**P(I) - 1))
         ENDIF
         WRITE(*, 55) P(I), F(I)
 10   CONTINUE
```

```
C
C:       Data output.
C
      OPEN (UNIT=9, FILE = 'f4.0.5')
C
      DO  20 J = 1, 25
        WRITE(9, 55)  P(J), F(J)
  20  CONTINUE
C
C
C:    TERMINATION:
C     -----------
C
 55   FORMAT (F6.3, 1X, F10.6)
C
      END
```

```
      PROGRAM  CVSKP
C
C
C   ****************************************************************
C   *                                                              *
C   *    TITLE:                  Steady State Concentration        *
C   *                                                              *
C   *    AUTHOR:                 Joanne Zhang                      *
C   *                                                              *
C   *    DATE Coded:             March  20, 1991                   *
C   *                                                              *
C   *    ORGANIZATION:           Chemical Engineering Department   *
C   *    LOCATION:               Bucknell University               *
C   *                            Lewisburg, PA   17837             *
C   *                                                              *
C   ****************************************************************
C
C:    PURPOSE:
C     -------
C
C          This program calculates the steady state ion concentration
C      either as a function of the aspect ratio k with potential
C      gradient p as a parameter or as a function of potential gradient
C      p with the aspect ratio k as a parameter.
C
C
C:    VARIABLES:
C     ---------
C
      REAL       K, KI(10)
      REAL       P, PI(13)
      CHARACTER  TYPE*1
      REAL       CK(10), CP(13), KK(20)
C
C
C:    INITIALIZATION:
C     --------------
C

C
C
C   ++++++++++++++++++++++++++++++++++++++++++++++++++++++++++++++++
C
C:    BODY:
C     ----
C
C:       Input parameters k and p.
C
c      PRINT*, ' Input the parameter (k or p, and RETURN for quit).'
c      READ*, TYPE
C
c      IF (TYPE .EQ. 'p')  THEN
         PRINT*, ' Input value of p: '
         READ*, P
C
      OPEN (UNIT = 9, FILE = 'f7.5')
C
C:       Calculate Ca/C0 as a function of k.
C
      PRINT*,
      PRINT*, '  K        Ca/C0 '
C
      DO 10  I = 1, 1000
         K = 0.2 + I*0.0001
         PP = (1-K)/(K*LOG(1/K))
         TOL = ABS(PP-P)
         IF (TOL .LT. 0.00001) GOTO 100
 10   CONTINUE
C
 100  CONTINUE
```

```
C
      DO 20  J = 1, 18
         KK(J) = J*K/20
c         KK(J) = KK(J)*3.5
C
         IF (J .EQ. 1) KK(J) = 0.01
C
         CK(J) = 1/(1 - P*KK(J)*LOG(1/KK(J))/(1-KK(J)))
C
C:       Data output
C
         WRITE(9, 55) KK(J), CK(J)
         WRITE(*, 55) KK(J), CK(J)
C
 20   CONTINUE
C
C
c      ELSEIF (TYPE .EQ. 'k')  THEN
c         PRINT*, ' Input value of k: '
c        READ*, K
C
C:       Calculate Ca/C0 as a function of p.
C
c         DO 30  I = 1, 13
c            IF (I .EQ. 13) THEN
c              PI(I) = 0.5
c            ELSE
c               PI(I) = (I-2)*1.0
c            ENDIF
c            CP(I) = 1/(1 - PI(I)*K*LOG(1/K)/(1-K))
c 30   CONTINUE
C
C:       Data output.
C
c         OPEN (UNIT = 19, FILE = 'cac0.k0.5')
C
c         PRINT*,
c         PRINT*, '  P        Ca/C0 '
C
c         DO 40  J = 1, 13
c            WRITE(19, 55) PI(J), CP(J)
c            WRITE(*, 55) PI(J), CP(J)
c 40      CONTINUE
C
c      ELSE
c        GOTO 100
c      ENDIF

C
C
C:    TERMINATION:
C     -----------
C
 55   FORMAT (1X, F6.3, 1X, F10.6)
C
c  200 CONTINUE
C
      END
```

```
      PROGRAM  CCPP
C
C
C   ****************************************************************
C   *                                                              *
C   *    TITLE:                  CA/C0 vs. P/P*                    *
C   *                                                              *
C   *    AUTHOR:                 Joanne Zhang                      *
C   *                                                              *
C   *    DATE Coded:             March  26, 1991                   *
C   *                                                              *
C   *    ORGANIZATION:           Chemical Engineering Department   *
C   *    LOCATION:               Bucknell University               *
C   *                            Lewisburg, PA   17837             *
C   *                                                              *
C   ****************************************************************
C
C
C:    PURPOSE:
C     -------
C
C          This program calculates the dimensionless ion concentration
C       CA/C0 as a function of the ratio of the potential gradient p
C       and its critical value p*.
C
C
C:    VARIABLES:
C     ---------
C
      INTEGER    N
      PARAMETER  (N = 51)
      REAL       CC(N), PP(N)
      REAL       P
C
C
C:    INITIALIZATION:
C     --------------
C

C
C
C   ++++++++++++++++++++++++++++++++++++++++++++++++++++++++++++++++
C
C:    BODY:
C     ----
C
      OPEN (UNIT = 9, FILE = 'f5.-0')
C
C:       Data calculation
C
      PRINT*,
      PRINT*, '   PP,      CC'
      DO 10  I = 1, 51
         P = 1.9/50.
         PP(I) = -1 + (I-1)*P
C
         CC(I) = 1/(1-PP(I))
C
C:       Data output
C
         WRITE(9, 55) PP(I), CC(I)
         WRITE(*, 55) PP(I), CC(I)
 10   CONTINUE
C
C
C:    TERMINATION:
C     -----------
C
 55   FORMAT (1X, F7.3, 1X, F10.3)
C
      END
```

```
      PROGRAM  PK
C
C
C   ****************************************************************
C   *                                                              *
C   *    TITLE:                  P* vs. K                          *
C   *                                                              *
C   *    AUTHOR:                 Joanne Zhang                      *
C   *                                                              *
C   *    DATE Coded:             March  26, 1991                   *
C   *                                                              *
C   *    ORGANIZATION:           Chemical Engineering Department   *
C   *    LOCATION:               Bucknell University               *
C   *                            Lewisburg, PA   17837             *
C   *                                                              *
C   ****************************************************************
C
C
C:    PURPOSE:
C     -------
C
C          This program calculates the critical value of potential
C       gradient p, p*, as a function of aspect ratio k.
C
C
C:    VARIABLES:
C     ---------
C
      INTEGER    N
      PARAMETER  (N = 101)
      REAL       K(N), PSTAR(N)
      REAL       KK1
C
C
C:    INITIALIZATION:
C     --------------
C

C
C
C   ++++++++++++++++++++++++++++++++++++++++++++++++++++++++++++++++
C
C:    BODY:
C     ----
C
      OPEN (UNIT = 11, FILE = 'fa6')
C
      PRINT*,
      PRINT*, '   K,          P*'
C
C:       Calcualte p* as a function of k.
C
      DO 10  I = 1, 101
         KK1 =  0.9/100
C
         IF (I .EQ. 100) THEN
            K(I) = 0.999
         ELSE
            K(I) = 0.1 + KK1*I
         ENDIF
C
         PSTAR(I) = (1-K(I))/(K(I)*LOG(1/K(I)))
C
C:       Data output.
C
         WRITE(11, 55) K(I), PSTAR(I)
         WRITE(*, 55) K(I), PSTAR(I)
 10   CONTINUE
```

```
C
C
C:    TERMINATION:
C     -----------
C
 55   FORMAT (1X, F7.3, 1X, F10.4)
C
      END
```

```
      PROGRAM  FINDAB
C
C
C   ********************************************************************
C   *                                                                  *
C   *    TITLE:                    FIND ALPHA AND BETA                 *
C   *                                                                  *
C   *    AUTHOR:                   Joanne Zhang                        *
C   *                                                                  *
C   *    DATE Coded:               April 10,  1991                     *
C   *                                                                  *
C   *    ORGANIZATION:             Chemical Engineering Department     *
C   *    LOCATION:                 Bucknell University                 *
C   *                              Lewisburg, PA   17837               *
C   *                                                                  *
C   ********************************************************************
C
C
C:    PURPOSE:
C     -------
C
C          This program evaluates the model constant ALPHA and BETA
C       by guessing ALPHA and BETA, calculating the variation (s**2)
C       of the theoretical value and the experimental data.  The best
C       values of ALPHA and BETA can be obtained by minimizing s**2.
C
C
C:    LOCAL CONSTANTS:
C     ---------------
C
      REAL        C0
      PARAMETER  (C0=11500)
      REAL        THATA
      PARAMETER  (THATA=336)
      INTEGER     N, M
      PARAMETER  (N = 26, M = 11)
C
C
C:    LOCAL VARIABLES:
C     ---------------
C
      REAL        ALPHA(N)
      REAL        CA(M), T(M)
      REAL        TPRIM(M), CAC0(M)
      REAL        S(N)
      REAL        LN(M)
C
C
C:    INITIALIZATION:
C     --------------
C
C
C   ++++++++++++++++++++++++++++++++++++++++++++++++++++++++++++++++++++
C
C:    BODY:
C     ----
C
C:       Read experimental data from data file.
C
      OPEN (UNIT=9, FILE = 'tca.dat')
C
      PRINT*,
      PRINT*, '   CAC0          TPRIM '
C
      DO 10  J = 1, M
         READ(9, *) T(J), CA(J)
         TPRIM(J) = T(J) - THATA
         CAC0(J) = CA(J)/C0
         PRINT*, CAC0(J), TPRIM(J)
 10   CONTINUE
```

```
C
C:       Input value of BETA.
C
      PRINT*,
      PRINT*, ' INPUT VALUE OF BETA: '
      READ*, BETA
C
C:       Find the best ALPHA.
C
      OPEN (UNIT = 11, FILE = 'alpha.dat')
      DO 20  I = 1, N
C
C:       Input value of ALPHA.
C
         READ(11, *) ALPHA(I)
c         PRINT*,
c         PRINT*, ' Input value of ALPHA: '
c         READ*, ALPHA(I)
C
C:       Calculate CA vs. TPRIM and S
C
      CALL  EQ(ALPHA(I), BETA, CAC0, T, TPRIM, S(I))
C
C:       Ask for next value of ALPHA.
C
  20  CONTINUE
C
C:       Write and store ALPHA, S in a data file.
C
      OPEN (UNIT = 29, FILE = 'ab.2.0')
C
      PRINT*,
      PRINT*, ' ALPHA,     S'
      DO 40  J =1, N
         WRITE(29, 44) ALPHA(J), S(J)
         WRITE(*, 44)  ALPHA(J), S(J)
 40   CONTINUE
C
C:    TERMINATION:
C     -----------
C
 44   FORMAT (1X, F6.2, 1X, F10 5)
C
      STOP
      END
C
C
      SUBROUTINE  EQ(AL, BETA, CAC0, T, TPRIM, SS)
C
      REAL       AL, BETA, SS
      REAL       TPRIM(13), CAC0(13)
C
      REAL       Y(13)
C
C:       Calculate Y by using ALPHA, BETA.
C
      SS = 0.0
      IF (AL .EQ. 0)  THEN
         DO 100  I = 1, 13
            Y(I) = BETA*TPRIM(I)
            SS = SS + (Y(I)-CAC0(I))**2
 100     CONTINUE
      ELSE
         DO 110  I = 1, 13
            Y(I) = (1/AL)*(1-EXP(-AL*BETA*TPRIM(I)))
            SS = SS + (Y(I)-CAC0(I))**2
 110     CONTINUE
      ENDIF
C
      RETURN
      END
```

```
      PROGRAM  NEWDATA
C
C
C   ***********************************************************************
C   *                                                                     *
C   *    TITLE:                    Theoretical Data Calculation           *
C   *                                                                     *
C   *    AUTHOR:                   Joanne Zhang                           *
C   *                                                                     *
C   *    DATE Coded:               April 30, 1991                         *
C   *                                                                     *
C   *    ORGANIZATION:             Chemical Engineering Department        *
C   *    LOCATION:                 Bucknell University                    *
C   *                              Lewisburg, PA   17837                  *
C   *                                                                     *
C   ***********************************************************************
C
C
C:    PURPOSE:
C     -------
C
C          This program calculates the theoretical data points by using
C       the best values of the model parameter Alpha and Beta.  The set
C       of theoretical data will be used to make a backplot of the
C       experimental data.
C
C
C:    CONSTANTS:
C     ---------
C
      REAL        ALPHA, BETA
      PARAMETER   (ALPHA =-0.462, BETA = 4.84E-3)
C
      REAL        C0
      PARAMETER   (C0 = 11500)
      REAL        THETA
      PARAMETER   (THETA = 288.)
C
      INTEGER     N
      PARAMETER   (N = 17)
C
C
C:    VARIABLES:
C     ---------
C
      REAL        CA(N), T(N)
      REAL        TL1, TL2, C1, C2
C
C
C:    INITIALIZATION:
C     --------------
C
C
C
C
C   +++++++++++++++++++++++++++++++++++++++++++++++++++++++++++++++++++++++
C
C:    BODY:
C     ----
C
      OPEN (UNIT = 15, FILE = 'old.dat')
      OPEN (UNIT = 16, FILE = 'new3.dat')
C
      PRINT*,
      PRINT*, '  T         CA'
C
      DO 10  I = 1, N
         READ(15, *) T(I)
         IF (T(I) .LT. 300)  THEN
            CA(I) = 0.
         ELSE
```

```
            IF (ALPHA .EQ. 0)  THEN
               CA(I) = C0*BETA*(T(I)-THETA)
            ELSE
               CA(I) = C0/ALPHA *(1-EXP(-ALPHA*BETA*(T(I)-THETA)))
            ENDIF
         ENDIF
C
         WRITE(*, 55)  T(I), CA(I)
         WRITE(16, 55) T(I), CA(I)
  10  CONTINUE
C
      TL1 = 850
      TL2 = 890
      IF (ALPHA .EQ. 0)  THEN
         C1 = C0*BETA*(TL1-THETA)
         C2 = C0*BETA*(TL2-THETA)
      ELSE
         C1 = C0/ALPHA *(1-EXP(-ALPHA*BETA*(TL1-THETA)))
         C2 = C0/ALPHA *(1-EXP(-ALPHA*BETA*(TL2-THETA)))
      ENDIF
C
      PRINT*,
      PRINT*, TL1, C1
      PRINT*, TL2, C2
C
C:    TERMINATION:
C     -----------
C
 55   FORMAT (1X, F6.0, 1X, F13.2)
C
      END
```

NIST-114A
(REV. 3-90)

U.S. DEPARTMENT OF COMMERCE
NATIONAL INSTITUTE OF STANDARDS AND TECHNOLOGY

BIBLIOGRAPHIC DATA SHEET

1. PUBLICATION OR REPORT NUMBER
NIST/TN-1293

2. PERFORMING ORGANIZATION REPORT NUMBER

3. PUBLICATION DATE
May 1992

4. TITLE AND SUBTITLE

A Mathematical Model of Cathodic Delamination and Blistering Processes in Paint Films on Steel

5. AUTHOR(S)

James Pommersheim, Tinh Nguyen, Zhuohong Zhang, Changjian Lin, and Joe Hubbard

6. PERFORMING ORGANIZATION (IF JOINT OR OTHER THAN NIST, SEE INSTRUCTIONS)

U.S. DEPARTMENT OF COMMERCE
NATIONAL INSTITUTE OF STANDARDS AND TECHNOLOGY
GAITHERSBURG, MD 20899

7. CONTRACT/GRANT NUMBER

8. TYPE OF REPORT AND PERIOD COVERED
Final

9. SPONSORING ORGANIZATION NAME AND COMPLETE ADDRESS (STREET, CITY, STATE, ZIP)

Same as item #6

10. SUPPLEMENTARY NOTES

11. ABSTRACT (A 200-WORD OR LESS FACTUAL SUMMARY OF MOST SIGNIFICANT INFORMATION. IF DOCUMENT INCLUDES A SIGNIFICANT BIBLIOGRAPHY OR LITERATURE SURVEY, MENTION IT HERE.)

Conceptual and mathematical models are developed for processes which describe blistering of defect-containing coating on coated steel containing defects exposed to electrolytic solutions. The assumption is made that cations migrating along the coating/metal interface from an anode at the defect to cathodic sites are responsible for blistering. The cations are driven by both concentration and electrical potential gradients. The mathematical models are solved to predict ion fluxes and concentrations along the interface and within the blister. Solutions of the models are expressed in terms of dimensionless parameters. Model variables include blister size, distance between the blister and defect, ion diffusivity and potential gradients. To substantiate the models , an experiment was designed and conducted to measure the transport of cations along the coating/metal interface from the defect to the blister. Sodium ion concentration-time data within a blister were analyzed to determine model parameters. Under the experimental conditions employed, it was found that the transport of sodium ions is controlled by potential gradients rather than concentration gradients. Model results indicate that large blisters subject to a potential gradient are more likely to grow than small ones because higher concentrations can build up within them. Implications of this conclusion for maintaining the integrity of organic coatings are discussed.

12. KEY WORDS (6 TO 12 ENTRIES; ALPHABETICAL ORDER; CAPITALIZE ONLY PROPER NAMES; AND SEPARATE KEY WORDS BY SEMICOLONS)

anode; blistering; cathode; cathodic delamination; conceptual model; corrosion; defect; diffusion; mathematical model; organic coatings; paint films; potential gradients; scribe

13. AVAILABILITY

X	UNLIMITED
	FOR OFFICIAL DISTRIBUTION. DO NOT RELEASE TO NATIONAL TECHNICAL INFORMATION SERVICE (NTIS).
X	ORDER FROM SUPERINTENDENT OF DOCUMENTS, U.S. GOVERNMENT PRINTING OFFICE, WASHINGTON, DC 20402.
X	ORDER FROM NATIONAL TECHNICAL INFORMATION SERVICE (NTIS), SPRINGFIELD, VA 22161.

14. NUMBER OF PRINTED PAGES
72

15. PRICE

ELECTRONIC FORM * U.S. G.P.O.:1992 311-891:60029

NIST Technical Publications

Periodical

Journal of Research of the National Institute of Standards and Technology—Reports NIST research and development in those disciplines of the physical and engineering sciences in which the Institute is active. These include physics, chemistry, engineering, mathematics, and computer sciences. Papers cover a broad range of subjects, with major emphasis on measurement methodology and the basic technology underlying standardization. Also included from time to time are survey articles on topics closely related to the Institute's technical and scientific programs. Issued six times a year.

Nonperiodicals

Monographs—Major contributions to the technical literature on various subjects related to the Institute's scientific and technical activities.

Handbooks—Recommended codes of engineering and industrial practice (including safety codes) developed in cooperation with interested industries, professional organizations, and regulatory bodies.

Special Publications—Include proceedings of conferences sponsored by NIST, NIST annual reports, and other special publications appropriate to this grouping such as wall charts, pocket cards, and bibliographies.

Applied Mathematics Series—Mathematical tables, manuals, and studies of special interest to physicists, engineers, chemists, biologists, mathematicians, computer programmers, and others engaged in scientific and technical work.

National Standard Reference Data Series—Provides quantitative data on the physical and chemical properties of materials, compiled from the world's literature and critically evaluated. Developed under a worldwide program coordinated by NIST under the authority of the National Standard Data Act (Public Law 90-396). NOTE: The Journal of Physical and Chemical Reference Data (JPCRD) is published bi-monthly for NIST by the American Chemical Society (ACS) and the American Institute of Physics (AIP). Subscriptions, reprints, and supplements are available from ACS, 1155 Sixteenth St., NW., Washington, DC 20056.

Building Science Series—Disseminates technical information developed at the Institute on building materials, components, systems, and whole structures. The series presents research results, test methods, and performance criteria related to the structural and environmental functions and the durability and safety characteristics of building elements and systems.

Technical Notes—Studies or reports which are complete in themselves but restrictive in their treatment of a subject. Analogous to monographs but not so comprehensive in scope or definitive in treatment of the subject area. Often serve as a vehicle for final reports of work performed at NIST under the sponsorship of other government agencies.

Voluntary Product Standards—Developed under procedures published by the Department of Commerce in Part 10, Title 15, of the Code of Federal Regulations. The standards establish nationally recognized requirements for products, and provide all concerned interests with a basis for common understanding of the characteristics of the products. NIST administers this program as a supplement to the activities of the private sector standardizing organizations.

Consumer Information Series—Practical information, based on NIST research and experience, covering areas of interest to the consumer. Easily understandable language and illustrations provide useful background knowledge for shopping in today's technological marketplace.

Order the **above** *NIST publications from: Superintendent of Documents, Government Printing Office, Washington, DC 20402.*

Order the **following** *NIST publications—FIPS and NISTIRs—from the National Technical Information Service, Springfield, VA 22161.*

Federal Information Processing Standards Publications (FIPS PUB)—Publications in this series collectively constitute the Federal Information Processing Standards Register. The Register serves as the official source of information in the Federal Government regarding standards issued by NIST pursuant to the Federal Property and Administrative Services Act of 1949 as amended, Public Law 89-306 (79 Stat. 1127), and as implemented by Executive Order 11717 (38 FR 12315, dated May 11, 1973) and Part 6 of Title 15 CFR (Code of Federal Regulations).

NIST Interagency Reports (NISTIR)—A special series of interim or final reports on work performed by NIST for outside sponsors (both government and non-government). In general, initial distribution is handled by the sponsor; public distribution is by the National Technical Information Service, Springfield, VA 22161, in paper copy or microfiche form.

U.S. Department of Commerce
National Institute of Standards and Technology
Gaithersburg, MD 20899